Behavioral/Cognitive

Circadian Modulation of Dopamine Levels and Dopaminergic Neuron Development Contributes to Attention Deficiency and Hyperactive Behavior

Jian Huang,[1,2]* Zhaomin Zhong,[1,2]* Mingyong Wang,[1,2] Xifeng Chen,[1,2] Yicheng Tan,[1,2] Shuqing Zhang,[1,2] Wei He,[1,2] Xiong He,[1,2] Guodong Huang,[1,2] Haiping Lu,[3] Ping Wu,[2] Yi Che,[2] Yi-Lin Yan,[1,4] ⦿John H. Postlethwait,[4] Wenbiao Chen,[1,5] and ⦿Han Wang[1,2]

[1]Center for Circadian Clocks, [2]School of Biology & Basic Medical Sciences, Medical College, [3]Department of Pediatrics and Child Health, Affiliated Children's Hospital, Soochow University, Suzhou 215003, Jiangsu, China, [4]Institute of Neuroscience, University of Oregon, Eugene, Oregon 97403, and [5]Department of Molecular Physiology and Biophysics, Vanderbilt University School of Medicine, Nashville, Tennessee 37232

Attention-deficit/hyperactivity disorder (ADHD) is one of the most prevalent psychiatric disorders in children and adults. While ADHD patients often display circadian abnormalities, the underlying mechanisms are unclear. Here we found that the zebrafish mutant for the circadian gene *period1b* (*per1b*) displays hyperactive, impulsive-like, and attention deficit-like behaviors and low levels of dopamine, reminiscent of human ADHD patients. We found that the circadian clock directly regulates dopamine-related genes *monoamine oxidase* and *dopamine β hydroxylase*, and acts via genes important for the development or maintenance of dopaminergic neurons to regulate their number and organization in the ventral diencephalic posterior tuberculum. We then found that *Per1* knock-out mice also display ADHD-like symptoms and reduced levels of dopamine, thereby showing highly conserved roles of the circadian clock in ADHD. Our studies demonstrate that disruption of a circadian clock gene elicits ADHD-like syndrome. The circadian model for attention deficiency and hyperactive behavior sheds light on ADHD pathogenesis and opens avenues for exploring novel targets for diagnosis and therapy for this common psychiatric disorder.

Key words: attention deficiency; circadian clock; dopamine; hyperactivity; *per1b*; zebrafish

Introduction

The circadian clock generates physiological and behavioral rhythms with a period of ~24 h and plays a critical role in the sleep/wake cycle (Dijk and von Schantz, 2005). Circadian dysfunctions are thought to underlie the pathogenesis of many psychiatric disorders, including mania-like behavior and bipolar disorder (McClung, 2013). Attention-deficit/hyperactivity disorder (ADHD; Online Mendelian Inheritance in Man #143465) is

one of the most prevalent psychiatric disorders in children and adults, affecting ~3–5% of the population (Geissler and Lesch, 2011). ADHD is characterized clinically by hyperactivity, inattention, and impulsivity (Kendall et al., 2008), which significantly impair normal development of academic and social functions in children, and lead to secondary problems, such as delinquency and drug addiction, in adults (Rösler et al., 2004). One of the key clinical manifestations of ADHD patients is obvious hyperactivity that in turn results in sleep deprivation (Philipsen et al., 2006). Genome-wide association studies (GWAS) of ADHD patients have implicated genes involved in the endogenous circadian clock as risk factors for ADHD (Lasky-Su et al., 2008). Mice carrying the dominant negative *Clock* mutation show mania-like behavior, including hyperactivity, decreased sleep, lowered depression-like behavior, reduced anxiety, and an increased reward value in association with elevated dopaminergic activities in the central tegmental area (McClung et al., 2005; Roybal et al., 2007), while the circadian nuclear receptor *Rev-erbα* (*Nr1d1*) knock-out mice also display mania-like behavior, particularly hyperactivity and a central hyperdopaminergic state (Chung et al., 2014). In addition, dysrhythmias of melatonin production and altered expression of the circadian clock genes *BMAL1* and *PER2* appear to be associated with adult ADHD patients (Baird et al., 2012). The mechanisms by which the circadian clock impacts the pathogenesis of ADHD, however, are far from certain.

The zebrafish (*Danio rerio*) has been validated as a model for studying the genetic and developmental bases of behaviors (Lieschke and Currie, 2007), and has demonstrated its superiority for high-throughput drug screens for behavioral disorders in whole organisms (Rihel et al., 2010). Here, we set out to establish a zebrafish circadian model for attention deficiency and hyperactive behavior and to investigate the regulatory roles of the circadian clock in ADHD. We showed that zebrafish mutants for the circadian gene *period1b* (*per1b*, an ortholog of human *PER1*) display hyperactivity, impulsivity-like and inattention-like behaviors, and low levels of dopamine (DA), reminiscent of human ADHD patients. This zebrafish model with altered circadian rhythms demonstrates that ADHD behaviors in humans, rodents, and zebrafish are all associated with a dysfunctional DA system. Per1b acts via enzymes critical for DA metabolism to directly regulate the endogenous DA levels, and also through genes critical for development of dopaminergic neurons to possibly regulate their number and spatial organization. We also determined that *Per1* knock-out mice display ADHD-like symptoms, reduced levels of DA, and disregulation of DA-related genes, thereby suggesting that the regulatory roles of Per1 in ADHD behaviors are conserved across vertebrates. The circadian models for attention deficiency and hyperactive behavior we describe provide insights into ADHD pathogenesis and should allow screens to identify novel targets for diagnosis and treatment for this common psychiatric disorder.

Materials and Methods

All procedures were approved by the Soochow University Animal Care and Use Committee and were in accordance with governmental regulations of China.

Fish husbandry and embryo production

Zebrafish, including a wild-type AB strain and *per1b* mutant lines, are raised at our fish facility according to standard protocols (Westerfield, 1993). Wild-type and mutant embryos were produced by pair matings, and then raised at 28.5°C in E3 embryo medium. To obtain larvae in the constant dark (DD) condition, embryos were first raised in the normal light/dark (LD, 14/10 h) condition for the first 3 d postfertilization (dpf) to activate and entrain the circadian system, and then transferred into the DD environment. For RNA isolation, embryos of different stages (every 4 h) were collected and then stored at −80°C. For *in situ* hybridization and immunofluorescence staining, embryos or larvae were fixed in 4% paraformaldehyde (PFA) in PBS for 3 h at room temperature (RT) or overnight at 4°C, then washed briefly with PBS, dehydrated, and stored in 100% methanol at −20°C until use.

Mutant generation and identification

The zebrafish *per1b* mutant was generated through a retroviral insertion approach (Golling et al., 2002), whereby the retroviral sequence was inserted into the first intron of the *per1b* gene. To identify *per1b* mutants, two pairs of PCR primers were used. As shown in Figure 2A, primers P1 and P2 flanking the insertion site were used to amplify an expected 430 bp PCR product specific to wild-type fish, while the mutant product would be >6 kb too long to be amplified with this primer pair. Primer P3, located in genomic DNA to the left of the insertion site, and primer P4, which is inside the retroviral sequence, were used amplify an expected 734 bp PCR product specific to the insertional mutant. Thus, homozygous mutants would have a single 734 bp band, wild-type fish a single 430 bp band, and heterozygous fish both bands (see Fig. 2B).

Quantitative real-time PCR

Using TRIzol reagent (Invitrogen), total RNAs were extracted from ∼50 of the homozygous *per1b* or wild-type larvae every 4 h from 48 to 140 h postfertilization (hpf) for the LD condition and 96–140 hpf for the DD condition, and other groups of larvae of specified stages or treatments. After treating with DNase, 3 μg of the purified total RNAs were reverse transcribed into cDNAs. Quantitative real-time PCR (qRT-PCR) was performed in an ABI StepOnePlus instrument with the SYBR green detection system (Invitrogen). PCR thermal profiles were 40 cycles with each cycle 10 s at 95°C and 30 s at 60°C. Experiments were performed in triplicates, each with three different biological samples (nine replicates) for corresponding genotypes and developmental stages. All results were normalized to the expression level of the housekeeping gene *β-actin*. qRT-PCR results are shown as a relative expression level calculated using the $2^{-\Delta\Delta CT}$ method (VanGuilder et al., 2008). *p* values were calculated with one-way ANOVA test or Student's *t* test.

Luciferase reporter assays

A 1698 bp (−1489 to +209 bp) fragment of the zebrafish *monoamine oxidase* (*mao*, ENSDARG00000023712) promoter region containing 6 E' boxes (CANNTG) or a 1403 bp (−1371 to +32 bp) fragment of zebrafish *dopamine β hydroxylase* (*dbh*, ENSDARG00000069446) promoter region containing 7 E' boxes was amplified and cloned into the luciferase reporter-containing vector pGL4.17 (Promega), and named as p*mao*-PGL4 and p*dbh*-PGL4, respectively. Full-length cDNAs of zebrafish *bmal1b* (ENSDARG00000035732), *clock1a* (ENSDARG00000011703), *clock2* (ENSDARG00000016536), *per1b* (ENSDARG00000016536), *cry1ab* (ENSDARG00000011583), and *cry1ba* (ENSDARG00000069074) genes (Kobayashi et al., 2000; Wang, 2008) were cloned into the pcDNA3.1 expression vector, respectively.

Real-time bioluminescence monitoring in transgenic fish

The two luciferase reporter constructs, p*dbh*-PGL4 and p*mao*-PGL4 (described above), were purified and linearized by NotI, and then microinjected into one-cell stage embryos for generating transgenic fish lines. Real-time bioluminescence of the F_1 transgenic larvae was monitored with a luminoskan ascent instrument (Thermo Fisher Scientific) using the dual-luciferase reporter assay system (Promega). The results were normalized by the CircWave (v3.3) software (Cho et al., 2012).

Cell culture and cotransfections

A mouse fibroblast cell line, NIH3T3, was used for cotransfection studies. Cotransfection and luciferase assays were performed according to the protocol described previously (Hampp et al., 2008).

Antibodies and chromatin immunoprecipitation

A peptide of 13 amino acids (PSSQLTQSPESDR) was selected from the Bmal1b protein sequence, synthesized, and used as an antigen to generate rabbit polyclonal antibody according to a standard protocol (Howard and Kaser, 2007). Peptides of 10 amino acids were selected. SEEPAHL-KEQ was selected from the Period2 protein sequence. ALKAGESAEV was selected from the Per1b protein sequence. These were used to generate mouse monoclonal antibodies according to a standard protocol (Howard and Kaser, 2007). Bmal1b, Per2, and Per1b antibodies were effective in Western blotting experiments. Bmal1b and Per2 antibodies were used in chromatin immunoprecipitation (ChIP) assays, while the Per1b and Per2 antibodies were used for immunofluorescence staining experiments.

For ChIP assays, a group of 200 wild-type larvae at 5 dpf was collected and cross-linked in 2% formaldehyde at RT for 30 min, then 1:10 v/v of 1.25 M glycine was added to stop cross-linking, followed by PBS washes (3×, each for 10 min). The following procedures were performed according to the manufacturer's protocol (Millipore's ChIP assay kit). We used purified rabbit or mouse IgG (Invitrogen) as a negative control. ChIP PCRs were performed using primers flanking the E' box sites as well as primers not flanking the E' box sites in the 5′ promoter regions of *dbh* and *mao* as controls.

Whole-mount in situ hybridization

Whole-mount *in situ* hybridization was conducted as described previously (Wang et al., 2007). Briefly, fixed larvae were incubated in 50% formamide hybridization buffer with a DIG-labeled RNA probe at 70°C for 18–20 h. Both nitro blue tetrazolium and 5-bromo-4-chloro-3-indolyl phosphate (Roche) were used for colorimetric detection. For each *in situ* hybridization experiment, 10–15 larvae were used. At least

three independent *in situ* hybridization experiments were conducted for each gene with an antisense *per1b* probe.

Western blotting analysis

Zebrafish larvae at 5 dpf were washed with fish water and homogenized in lysis buffer as described previously (Wang et al., 2011). Protein samples were separated with 8% SDS-PAGE and transferred to PVDF membranes. After blocking with 5% nonfat milk for 2 h, PVDF membranes were incubated with primary antibody overnight at 4°C. The next day, membranes were washed in TBST (0.5% Tween 20) three times, each for 10 min, and then incubated for 4 h with anti-mouse or anti-rabbit HRP-conjugated secondary antibody (1:5000; Abcam) at 4°C. After washing with TBST four times, 10 min each, membranes were detected by a chemoluminescent HRP substrate (Thermo Fisher Scientific).

Immunofluorescence staining with tyrosine hydroxylase antibody

A group of 12 5 dpf zebrafish larvae were used to perform tyrosine hydroxylase (TH) immunofluorescence staining. Fixed larvae were placed in 30% sucrose in PBS overnight and then transferred to Tissue-Tek O.C.T. and stored at −26°C. Sections with a thickness of 16 μm were prepared using a cryostat (Leica CM1850). Immunofluorescence was performed as follows: slides with sections were washed with PBS (3×, each for 10 min), followed by PBST (3×, each for 10 min), and finally PBS plus 0.5% Triton X-100 (2×, each for 5 min). Sections then were blocked in 3% bovine serum albumin in PBS for ≥30 min and incubated with TH primary antibody (mouse, 1:1000; Immunostar) overnight at 4°C. The following day, sections were washed with PBS (3×, each for 10 min) and PBS plus 0.1% Triton X-100 (2×, each for 5 min). Sections were then incubated with secondary antibody (anti-mouse Alexa 488; A21202, Invitrogen) for 2 h, followed by washing with PBS (6×, each for 10 min). Slides were coverslipped using DAPI solution (Vector Lab, H1200). Images were taken using a Zeiss compound microscope (Axio Imager M2) with a digital camera and processed using Adobe Photoshop CS. A double-blind test was used to calculate the number of dopaminergic neurons in the ventral diencephalic posterior tuberculum (PT).

Immunostaining of the mouse brain was performed as described previously (Gong et al., 2011). Two-month-old mice were overdosed with pentobarbital and perfused with saline followed by 4% paraformaldehyde. The fixed brain was cryoprotected in 30% sucrose, and cut into 20 μm coronal sections on a cryostat (Leica CM1850). Sections were incubated with a mixture of two primary antibodies (mouse anti-TH, 1:1000; Immunostar; and rabbit anti-PER1, 1:600; Abcam, ab3443) overnight at 4°C. After washing with PBS three times, sections were then incubated with a mixture of secondary antibodies (anti-mouse Cy3 conjugated, 1:1000; Invitrogen; and anti-rabbit Alexa 488 conjugated, 1:1000; Invitrogen) for 2 h at RT. After washing with PBS three times, sections were coverslipped with DAPI solution (Vector Lab, H1200).

HPLC analysis

Measurement of endogenous DA concentrations was performed at the Institute of Basic Chinese Medical Theory, China Academy of Chinese Medical Sciences. The protocol was performed as described previously (Lange et al., 2012). Brains of 12 adult fish (5–6-month-old) were dissected out at Zeitgeber time (ZT) 1 and ZT15 and fast frozen in liquid nitrogen, then stored at −80°C until use. Approximately 100 larvae were fast frozen each at ZT2 (98 and 122 hpf) and ZT14 (110 and 134 hpf). Samples were stored at −80°C until use. For HPLC analysis, ~100 zebrafish (≥50 mg) larvae or 50 mg adult brains were homog-
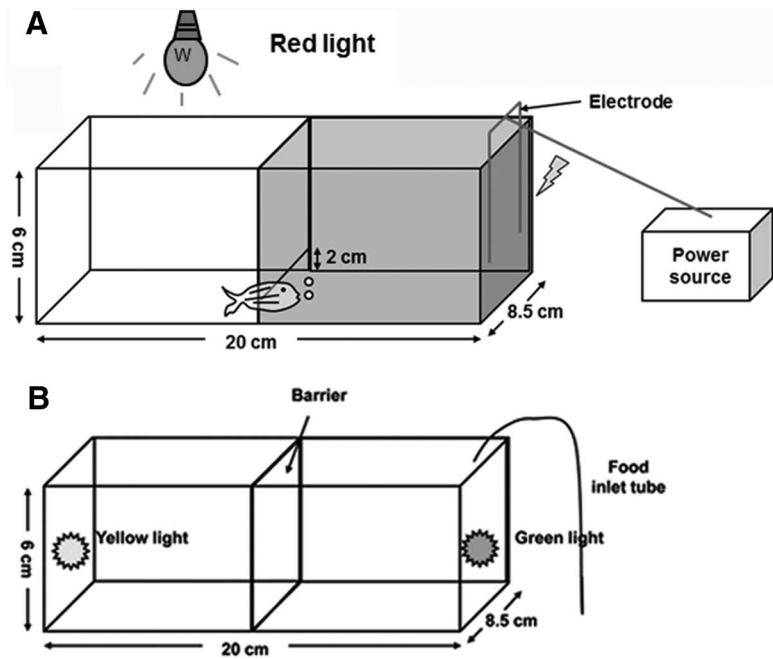

Figure 1. Testing tanks for the escape assay and food reward with a two-choice, serial reaction-time task assay. Tanks were made of plastic, as was the barrier, and relative size is depicted in the picture. ***A***, The right half of the tank was covered with opaque paper, which mimics a dark box. The left part of the tank mimics a light box. An electric pulse was turned on as soon as the fish entered the dark side of the tank. ***B***, Lights comprised 1× yellow and 1× green LEDs (3V) controlled by the experimenter with an externally located switch box. The food inlet tube was attached on the left side near the green LED.

enized in 250 μl of 0.1 M acetic acid containing 10 μM EDTA, ascorbic acid, and sodium metabisulfite. Samples were stored at −80°C until analysis. Measurements of neurotransmitters, including DA, homovanillic acid (HVA), 3,4-dihydroxyphenylacetic acid (DOPAC), norepinephrine (NE), 5-hydroxyindoleacetic acid (5-HIAA), were performed on a Varian Polaris Programmable Binary Gradient HPLC System (Agilent Technologies). Reagents were purchased from Sigma-Aldrich. Calibration curves were obtained by injecting standard samples (DA, Sigma-Aldrich, H8502; HVA, Sigma-Aldrich, H1252; DOPAC, Sigma-Fluka, 11569; 5-HIAA, Sigma-Aldrich, H8876) of five different concentrations (5, 10, 20, 40, and 80 ng/ml). Correlation coefficients were >0.999.

Zebrafish behavioral analysis

Long-term monitoring of locomotor activity. Locomotor activity analysis was performed as described previously with some modifications (Prober et al., 2006). On the fourth dpf, a single larva was placed in each of 72 wells of a 96-well plate (36 wild types and 36 *per1b* mutants), which allowed simultaneous tracking of each larva. Locomotor activities of larvae were monitored for 4 consecutive days under the LD conditions using an automated video-tracking system (Videotrack, ViewPoint Life Sciences; or DanioVision Tracking System, Noldus Information Technology), and the movement of each larva was recorded and analyzed using Zebralab3.10 software (ViewPoint Life Sciences) or Ethovision 10.0 software (Noldus Information Technology). Ninety-six-well plates were placed inside the Zebrabox/DanioVision Observation Chamber where continuous infrared light was illuminated and white light was illuminated from 9:00 A.M. to 11:00 P.M. Instruments were placed in the chamber to maintain a constant temperature of 28.5°C. The Videotrack quantization parameters were set as described previously (Appelbaum et al., 2010). The test was performed ≥3 times. Data were further analyzed using custom R language and Visual Basic Macros for Microsoft Excel.

For the DD assay, live video tracking and analysis were conducted using Ethovision 10.0 software (Noldus Information Technology). The *per1b* mutant and wild-type embryos were kept under LD conditions for the first 3 d of development. On the fourth dpf, the mutant and wild-type larvae (48 each) were placed in a 96-well plate, which then was loaded inside the observation chamber of the DanioVision Tracking System (Noldus Information Technology). The temperature of the chamber was

maintained at 28°C by a temperature control unit (Noldus Information Technology). The light was set at 300 lux during daytime of 4 dpf, 0 lux during nighttime of 4 dpf, and then at 30 lux for all subsequent days for the DD condition starting from 9:00 A.M. at 5 dpf. Activities were measured from days 5 to 10 postfertilization, and swimming distances of the larvae were recorded in 10 min time bins (Tovin et al., 2012; Ben-Moshe et al., 2014). Locomotor activities under DD conditions were repeated four times, and the data were calculated with Student's t test using SPSS. Each value was shown as mean ± SEM, considering $p < 0.05$ as statistically significant. The period, amplitude, and phase were reanalyzed using a nonlinear least-squares minimization method (Pendergast et al., 2012; Liu et al., 2014). Activity levels that were above the 24 h average were plotted relative to the peak activity level in each actogram; activity levels below the 24 h average were set to zero (Hurd et al., 1998).

For the locomotor activity assay in adult fish, male or female adult fish were placed in 1 L tanks (20 × 8.5 × 6 cm) and transferred to the experiment room. All sides of the tank were covered by opaque tape to prevent external interference. After 1 h of acclimation, fish were placed in tanks containing system water to a depth of 6 cm, and activities were measured. Using the same procedure for larval locomotor activity, swimming activities were monitored over 2 h by counting the swimming distance every 5 min, for a total of 20 observation bins.

Active-avoidance conditioning paradigm for learning and memory ability analysis. The test was performed as described previously (Rawashdeh et al., 2007). Adult male zebrafish, 6–7 months of age, with an average length of ∼3 cm, were trained on an active-avoidance conditioning (AAC) paradigm using a modified testing tank [dimensions, 20 (length) × 8.5 (width) × 6 (height); water level, 5 cm]. This testing tank had an opaque barrier with an underwater opening to allow passage. The barrier divided the tank into two compartments of equal size; the right compartment was covered with dark, opaque paper to form a dark area. An electrode was installed at the right end of this area (Fig. 1A). Animals had to cross the barrier to avoid electric shocks (50 mA; pulse duration, 10 s; interpulse amplitude, 500 ms; Fig. 1A). Before the test, the room light was turned off, with dim red light illuminating the left part of the testing tank. All the fish were placed individually in 1 L tanks and transferred to the experiment room for ≥1 h for acclimation. Before training began, fish were first put into the left part of the testing tank one by one, and nearly all the fish passed through the barrier to the dark part in 10 s. Fish that did not go to the dark part in 10 s were excluded from the test. During the training period, the electric pulse was switched on as soon as the fish entered into the dark part (Fig. 1A, right compartment). Animals could learn to avoid the shock by swimming into the illuminated part within the first 10 s of each trial. Training was terminated once the animal was able to stay in the illuminated part for >10 s, and the time points of the electric pulse were recorded. The learning criterion was defined as staying correctly in the left, illuminated portion for >10 s in 8 of 10 consecutive trials during the training period without returning to the dark compartment. Animals that did not achieve the criterion for learning ability within 30 min after the onset of training were excluded from the experiment. Testing at defined intervals (24 h) was used to estimate long-term memories. The test was performed at ZT8 (daytime) and ZT16 (nighttime).

Evaluation of retention. To quantitatively evaluate the ability of each learner to recall the AAC paradigm, a retention score (RS) was calculated using the following algorithm (Rawashdeh et al., 2007):

$$RS = \frac{(time^{train} - 8) - (time^{test} - 8)}{(time^{train} - 8) + (time^{test} - 8)}$$

Training time required to reach the learning criterion in the test session was subtracted from the training time required to form the learning ability in the training session, divided by the training time in the test-plus-training sessions.

Reward-mediated impulsivity evaluation. This test was performed as described previously (Parker et al., 2012). All behavioral testing took place in a custom-built tank. The tank was constructed from a translucent, nonreflective acrylic box [6 (height) × 8.5 (width) × 20 cm (length); Fig. 1B], fitted with opaque barriers to form the response aper-

tures and the food-magazine areas. The tank was filled with 3 L of system water. A high-speed camera (Videotrack, ViewPoint Life Sciences) was placed above the box to facilitate continuous real-time observation and recording of the fish in the test tank.

Before training, fish were not fed for 3 d and then were transferred into the testing tank without a barrier. The yellow and green LEDs were switched on to see whether the fish had color preference. We selected fish without color preference for further examination. During the training period, the barrier was added, and 5–10 live brine shrimps were injected near the green light 5 s after it was switched on to form a reward-stimulus system, then we put the fish into another part of the tank with the yellow LED switched on, but no brine shrimp were injected. Each fish was trained and tested separately. After consecutive daily trainings for a week, fish that had already formed a reward memory were selected to perform the test experiment. As a result, 36 fish for each genotype were selected.

During the test period, the barrier was taken away, and both LEDs were switched on. However, no brine shrimp were injected until 4 min later. Fish that entered the right region (4 × 4 cm region near the green light) and remained near the region for 10 s were regarded as "correct fish"; fish that never entered the region were considered as "incorrect fish"; and fish that entered the region but stayed <5 s were identified as "omission fish."

Mirror-image attack test. The same tank used in the locomotor activity assay for adult fish was used for the mirror-image attack test, except that an 8 × 8 cm mirror was placed outside one side of the tank. The numbers of times adult fish attacked the side with the mirror were recorded with the same automated video-tracking system mentioned above (see Movie 2).

Activities in light and dark as a measure of environmental sensitivity. The Zebrabox was illuminated with 90 s light/dark cycles (300 lux during illumination) and the locomotor activities of larvae were monitored as described above.

Drug treatments. All drug solutions were freshly prepared with system water on the day of the experiment. A group of 6-dpf-old larvae were incubated in drug solution with 5, 10, 15, or 20 μM of deprenyl (Sigma-Aldrich) or 5, 10, 15, 20, or 40 μM of methylphenidate (MPH; Sigma-Aldrich), respectively, for 1 h to find an optimal concentration. The distance swum during a 5 min period was recorded for the different treatments as described above. Twenty-four wild-type larvae and 24 *per1b* mutant larvae were incubated in the optimal concentration in a 48-well plate for 1 h, and the distance swum within 5 min was determined from the recording.

To determine the effect of Ritalin on mirror-attacking behavior, 8-month-old mutant male and wild-type male fish were adapted to the testing room for 2 d without feeding, each housed in a 1.5 L tank containing 1 L system water. On the third day (1–5:30 P.M.), a mirror was placed outside one end of the tank and mirror-attacking behavior was monitored for 5 min. On the fourth day, Ritalin was added to half of the fish tanks for each group to a final concentration of 100 μM, while the others were left alone. Mirror-attacking behaviors were monitored 1 h post-treatment. Total swimming distances and times of attacking the mirror side of the treated fish and untreated control fish were recorded within 5 min.

Mouse behavior analysis
The behavior analysis (open field, Morris water maze) for wild-type C57/B6 and *Per1* (strain name: B6.129-*Per1^{tm1Drw}*/J, http://jaxmice.jax.org/strain/010491.html; Bae et al., 2001) knock-out mice was performed as described previously (Gunn et al., 2011).

Results

Generation of a *per1b* mutant
We generated a zebrafish mutant for the circadian clock gene *per1b* using a retroviral insertion approach (Golling et al., 2002), and found that the retroviral sequence was inserted into the first intron (Fig. 2A,B). A previous study showed that a viral insertion into the first intron before the start codon usually results in abnormal mRNA processing (Harbers et al., 1984). To test the hypothesis that the expression level of *per1b* mRNA is affected by
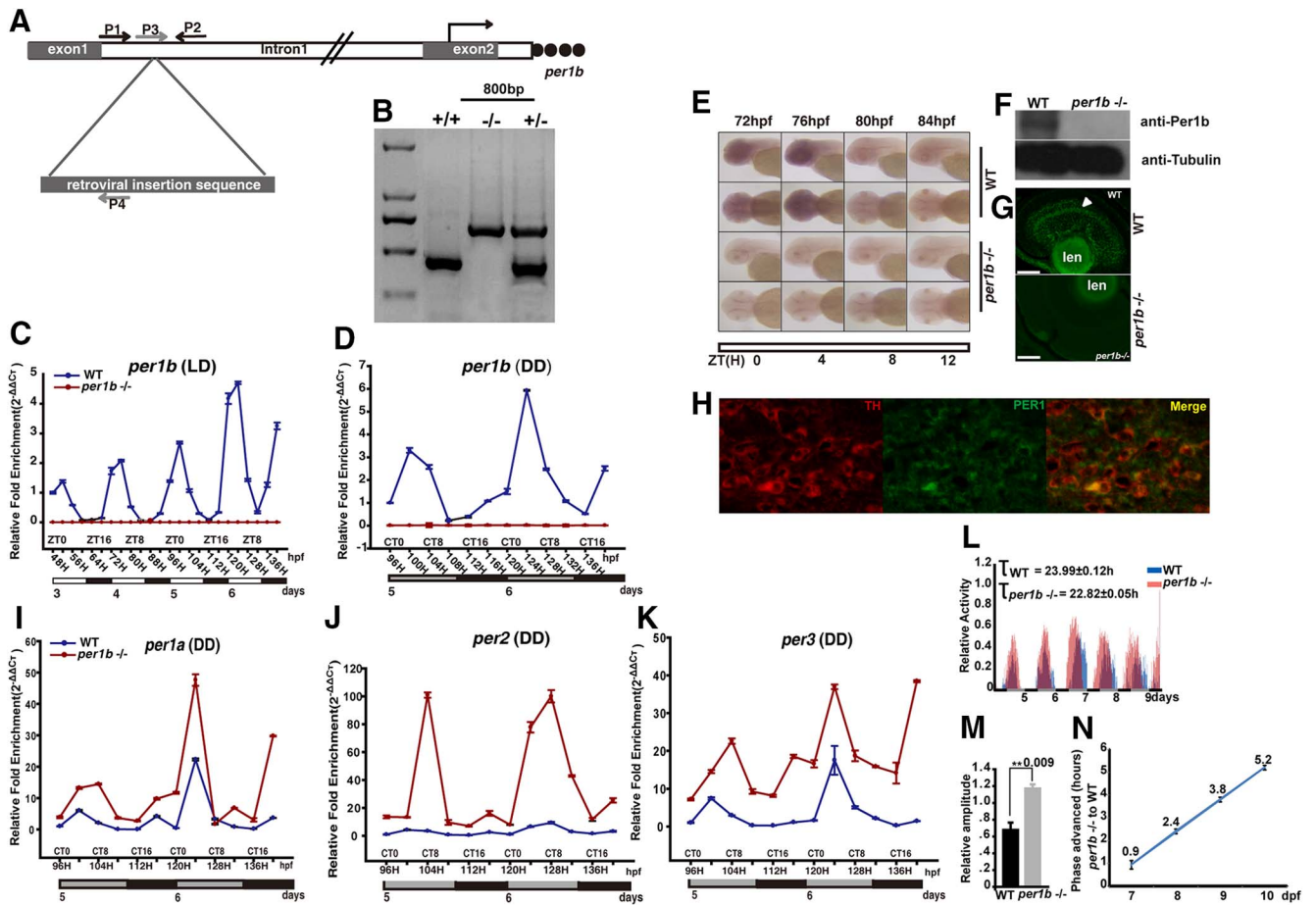
Figure 2. Identification of a zebrafish *per1b* insertional mutant. *A*, *B*, Insertion of the retroviral sequence into the first intron of zebrafish *per1b*. Arrows show the locations of PCR primers used to identify homozygous *per1b* mutants, heterozygotes, or wild-type fish. *C*, *D*, qRT-PCR analysis showed that *per1b* is rhythmically expressed in wild-type fish but its expression is nearly abolished in homozygous *per1b* mutants under both LD and DD conditions. One-way ANOVA test. Error bars are ±SEM. *E*, Whole-mount *in situ* hybridization experiments showed rhythmic expression of *per1b* in wild-type fish, but abolition of *per1b* expression in homozygous mutants under LD conditions. *F*, The homozygous *per1b* mutant lacks the Per1b protein. Proteins were extracted from wild-type and *per1b* mutant brains and eyes. Western blotting was done with tubulin antibody as an internal control. *G*, Immunofluorescence staining of Per1b indicated that the Per1b protein is primarily expressed in the inner nuclear layer of the retina (white arrow) and there is no detectable signal in the *per1b* mutant. Scale bar, 40 μm. *H*, Colocalization of the PER1 (green) and TH (red) proteins in dopaminergic neurons in the SN of mice, shown by immunofluorescence. Scale bar, 100 μm. *I*–*K*, Under DD conditions, *per1a* (*I*), *per2* (*J*), and *per3* (*K*) are all upregulated in *per1b* mutant zebrafish during both subjective daytime and nighttime. Expression ratios were normalized according to β-actin (RTPrimerDB ID:705) as an internal control using the $2^{-\Delta\Delta CT}$ method, and analyzed by one-way ANOVA test. *L*, Homozygous *per1b* mutants (5–10 dpf) exhibited ∼1.2 h shorter period under DD conditions. *M*, The relative amplitude of *per1b* mutants was significantly higher than wild types under DD conditions. Wild-type larvae, $n = 48$; *per1b* mutant larvae, $n = 48$. Student's *t* test. *N*, The *per1b* mutant displays a phase-advanced phenotype compared with wild types under DD conditions. The average time advanced was ∼2 h. Wild-type larvae, $n = 48$; *per1b* mutant larvae, $n = 48$. The number on the right side of the star indicates the *p* values.

this type of retroviral integration, we performed qRT-PCR, semi-quantitative RT-PCR, and whole-mount *in situ* hybridization. Results showed that wild types expressed *per1b* rhythmically under both LD and DD conditions, but that homozygous *per1b* retroviral insertion mutants showed only ∼10% of the wild-type *per1b* transcript levels (Fig. 2C–E). Western blotting with a Per1b monoclonal antibody showed a barely detectable signal in the *per1b* mutant but substantial signal from wild types (Fig. 2F), thus verifying the effect of the mutation on Per1b production. Immunofluorescence staining with the same antibody indicated that in wild types, the Per1b protein was expressed primarily in the eye, particularly in the inner nuclear layer of the retina, while in *per1b* mutants, little signal was detected (Fig. 2G). These results strongly indicate that the insertion mutant of *per1b* is likely a null-activity mutant. Furthermore, immunostaining demonstrated colocalization of the PER1 protein and TH in the dopaminergic neurons of the wild-type mouse brain substantia nigra (SN) region, which controls motivation and reward behaviors (Fig. 2H), suggesting that Per1 functions in dopamin-

ergic neurons. We were unable to detect Per1b protein expression, however, in zebrafish dopaminergic neurons (data not shown), likely due to its low expression levels or a suboptimal antibody.

Zebrafish has four *period* genes: *per1a* and *per1b*, which are both co-orthologs of mammalian *Per1*; and *per2* and *per3*, which are single orthologs of mammalian *Per2* and *Per3* (Wang, 2008). Under DD conditions, *per1a*, *per2*, and *per3* were all significantly upregulated in *per1b* mutants during both the subjective daytime and the subjective nighttime (Fig. 2I–K), indicating that Per1b serves as a negative regulator of the three other *period* genes in the zebrafish circadian system. Intriguingly, under DD conditions, we found that the *per1b* mutant larvae displayed an ∼1.2 h shortened circadian period in comparison with wild types (Fig. 2L), consistent with an ∼1 h shorter period found in *Per1* knock-out mice (Cermakian et al., 2001). The locomotor amplitude of the *per1b* mutant larvae was significantly higher than that of wild-type controls under DD conditions (Fig. 2M). Furthermore, the *per1b* mutant larvae showed a phase-advanced phenotype with
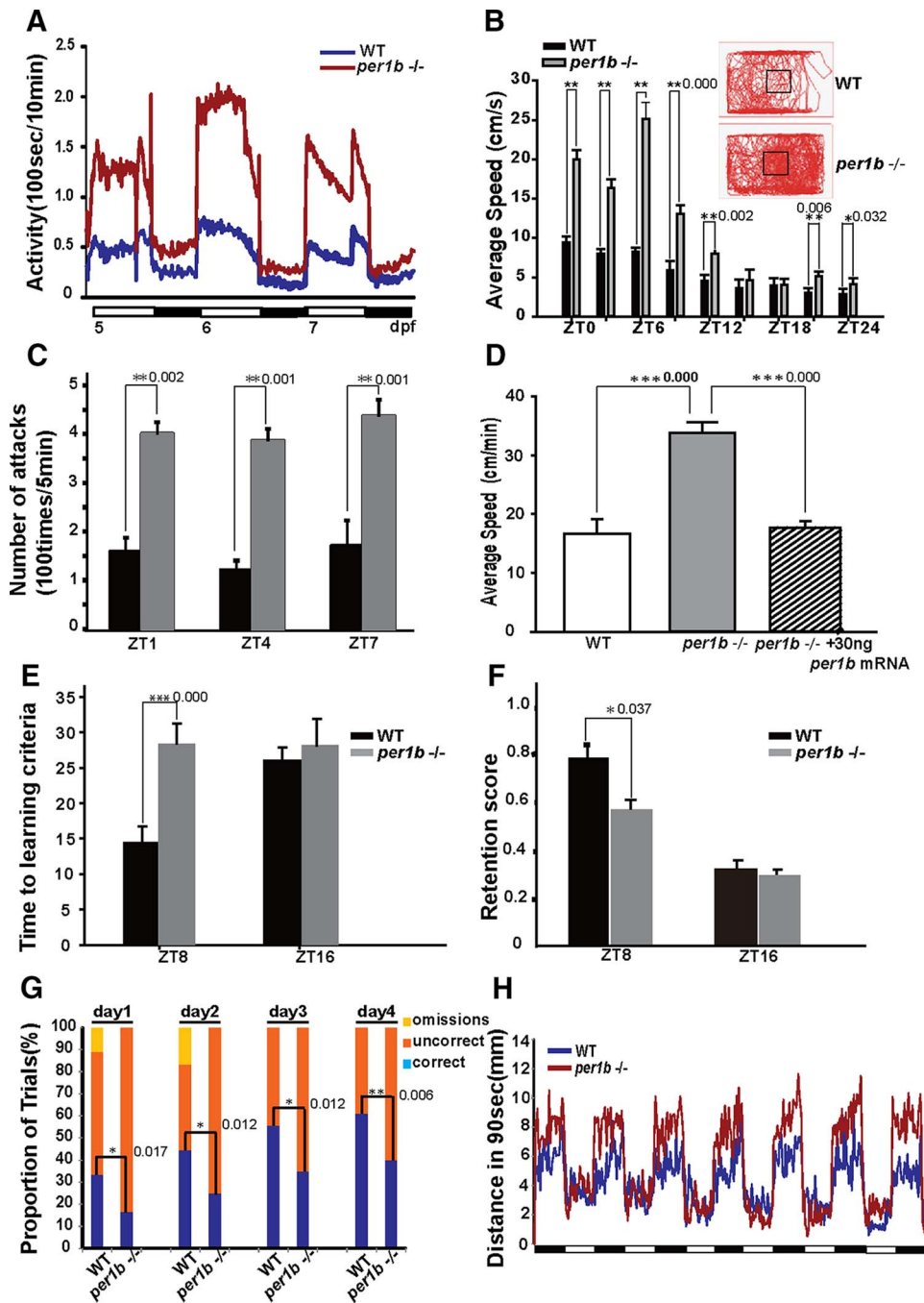
Figure 3. Homozygous *per1b* mutant zebrafish display ADHD-like behaviors. *A*, The *per1b* mutant larvae display hyperactive locomotor behaviors under LD conditions. Mean locomotion time was monitored in 5–7 dpf larvae. *per1b* mutant, $n = 36$; wild type, $n = 36$. Student's *t* test. *B*, The *per1b* mutant adults display hyperactive locomotor behaviors under LD conditions. Mean average swimming velocities of *per1b* mutant and wild-type adult zebrafish at time-of-day points under LD conditions (bars), and the accumulative total tracks of the *per1b* mutant and wild-type adult fish under LD conditions (rectangles). In addition to overall higher locomotor activities, *per1b* mutant adults appear to exhibit relatively higher locomotor activities in the center of the tank than the wild-type fish (squares in the center), indicating a less centrophobic and anxious phenotypes in the *per1b* mutant adult fish. Error bars are ±SEM. *per1b* mutant, $n = 12$; wild type, $n = 12$. Student's *t* test (Movie 1). *C*, Hyperactivity and impulsive-like behavior of the *per1b* mutant fish, shown by the mirror-image attack assay. *per1b* mutant, $n = 18$; wild type, $n = 18$. Error bars are ±SEM. Student's *t* test (Movie 2). *D*, Hyperactivity of *per1b* mutant larvae can be rescued by microinjection of functional *per1b* mRNAs. Thirty nanograms of capped *per1b* mRNAs were injected into one-cell *per1b* mutant embryos and locomotor activities were monitored from 5 to 7 dpf. Error bars are ±SEM. *per1b* mutant, $n = 36$; wild type, $n = 36$; *per1b*-injected embryos, $n = 36$. Student's *t* test. *E*, Adult *per1b* mutant fish showed significant learning problems in the AAC paradigm. The *per1b* mutant fish required more trials than wild types to learn to avoid electric shocks in the daytime (ZT8). *F*, The performance of *per1b* mutant fish in the memory test was inferior to that of wild types during the daytime. Error bars are ±SEM. *per1b* mutant, $n = 12$; wild type, $n = 12$. Student's *t* test. *G*, *per1b* mutant fish showed impulsivity-like symptoms determined by a food reward assay with the two-choice serial reaction-time task (see Materials and Methods). Correct (blue bars), incorrect (orange bars), and omission (yellow bars) results were marked with different colors. *per1b* mutant, $n = 24$; wild type, $n = 24$. *H*, A short-period (90 s each) light-pulse test showed that *per1b* mutant larvae are more sensitive to rapid changes in the illumination environment than wild-type controls. A 90 s light/dark pulse cycle was programed to the testing chamber holding 6 dpf larvae, and swimming distance during each cycle was monitored. *per1b* mutant, $n = 36$; wild type, $n = 36$. All the numbers on the right side of the star indicate the *p* values.
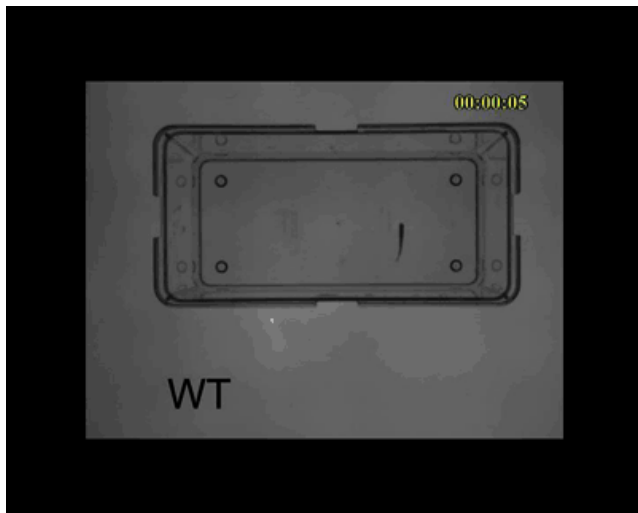
Movie 1. Hyperactivity of *per1b* adult mutant zebrafish. In comparison with wild types, *per1b* adult mutant zebrafish swam much faster and moved longer distances in the same time interval.
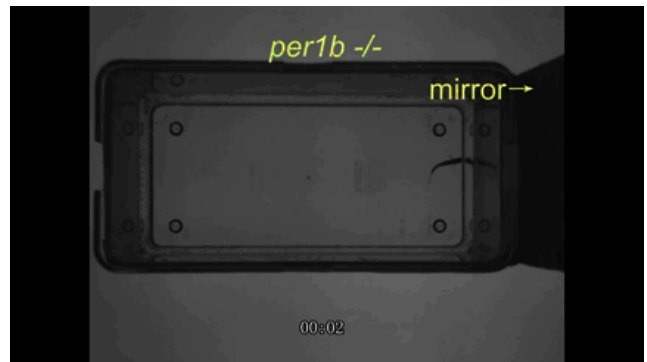

Movie 2. Impulsivity of *per1b* adult mutant zebrafish and its rescue by Ritalin treatment, determined by the mirror-image attack assay. Wild-type zebrafish attacked their mirror image, then broke off and attacked their mirror image again, while the *per1b* mutant zebrafish constantly attacked their mirror image, rarely breaking off (see text for discussion). The attacking times of *per1b* adult mutant fish are significantly reduced following 1 h 100 μM Ritalin treatment.

an average time of 2 h under DD conditions (Fig. 2*N*), similar to patients with familial advanced sleep phase syndrome due to a mutation in human *PER2* (Toh et al., 2001). These results show that Per1b is essential for zebrafish circadian regulation.

per1b mutant fish display hyperactive behavior

We then further analyzed zebrafish locomotor activities under LD conditions and found that 5–7 dpf *per1b* mutant larvae were ~3 times more active than their wild-type counterparts during both daytime and nighttime (Fig. 3*A*). We also measured swimming velocities of adult fish. Similar to larvae, the mean swimming speed of *per1b* mutant adult fish was approximately twice that of wild-type fish during the daytime and nearly one and a half times the wild-type value during the nighttime (Fig. 3*B*; Movie 1). We conclude that *per1b* mutant larvae and adult fish both exhibit hyperactivity. In addition, we also observed that the *per1b* mutants were less centrophobic than wild-type fish (Fig. 3*B*, rectangles). In other words, the *per1b* mutants displayed a dramatically increased exploratory behavior, implicating a reduced anxiety phenotype (Roybal et al., 2007).

We also used an image-attack assay (Bolyard and Rowland, 1996) to examine "perseveration," a key diagnostic criterion for hyperactivity in ADHD. High-speed camera monitoring showed that during the daytime (ZT1, ZT4, and ZT7), wild-type fish attacked their image intermittently in a 10 min interval. Wild-type fish would attack several times for a short period and then break off the attack, leave the mirror, and swim to other regions of the tank, and only resume attacking when they happened to see their image again. In contrast, *per1b* mutant fish attacked their mirror image nearly continuously in a 10 min period, failing to break off the attack as wild-type fish did. Thus the adult *per1b* mutant fish also displays perseveration-like behavior, shown by their persistently swimming toward the mirror side of the tank during the test (Fig. 3*C*; Movie 2).

To ensure that observed hyperactivity is caused by the *per1b* mutation rather than some other closely linked genetic aberration, we performed rescue experiments by microinjecting *per1b* capped mRNAs into one-cell zebrafish embryos. Results showed that hyperactivity of 5–7 dpf mutant larvae was rescued by *per1b*

functional mRNAs (Fig. 3*D*). We conclude that the viral insertion into the *per1b* gene is responsible for the behavioral abnormality.

per1b mutant fish show learning-deficit and memory-deficit behaviors

Next, we investigated the attention-deficit phenotype that also characterizes human ADHD patients. Recognizing that attention is particularly difficult to translate into defined behaviors in animal models and that distractibility and carelessness cannot easily be measured in such systems (Alsop, 2007), we focused on behaviors mimicking the forgetfulness and the trouble remembering obligations or appointments that are typical symptoms in both children and adult ADHD patients (Pastor et al., 2008). A well established methodology for examining learning and memory in adult fish is the AAC paradigm, in which one measures the ability of fish to learn and remember to avoid an electric shock by moving away from a naturally preferred dark area (but now an unsafe, shock-prone environment) into a naturally less favored light area (but now a safe, shock-free environment) of the tank (Fig. 1*A*; see Materials and Methods; Rawashdeh et al., 2007). We assessed this behavior in 2 consecutive days at two time-of-day points, ZT8 (daytime) and ZT16 (nighttime). During the training stage, at ZT8 in the daytime *per1b* mutants needed ~28 ± 2.8 trials to learn to avoid the electric stimulus to criterion (see Materials and Methods), while wild-type controls needed only half as many trials (14 ± 2.4 trials). We conclude that *per1b* mutants are not able to learn as well as wild types. At ZT16 in the nighttime, however, wild-type controls and *per1b* mutants showed no significant difference, indicating that the *per1b* mutants have less ability to learn or focus on a special task, but only in the daytime (Fig. 3*E*).

During the test stage in the following day, we estimated the memory of fish using the RS (as described in Material and Methods), which reflects the ratio between training and testing performances. We observed that during the daytime at ZT8, *per1b* mutant fish showed a decreased ability to acquire and remember the AAC stimulus compared with wild-type fish, while no significant difference in memory acquisition or retention between wild-type controls and *per1b* mutants appeared during the nighttime at ZT16 (Fig. 3*F*). This result suggests that *per1b* mutant fish have a lower ability to form long-term memories than wild-type fish ($n = 36$, t test, $p < 0.05$). We conclude that *per1b* mutant fish show a clear deficit in learning and memory ability, which
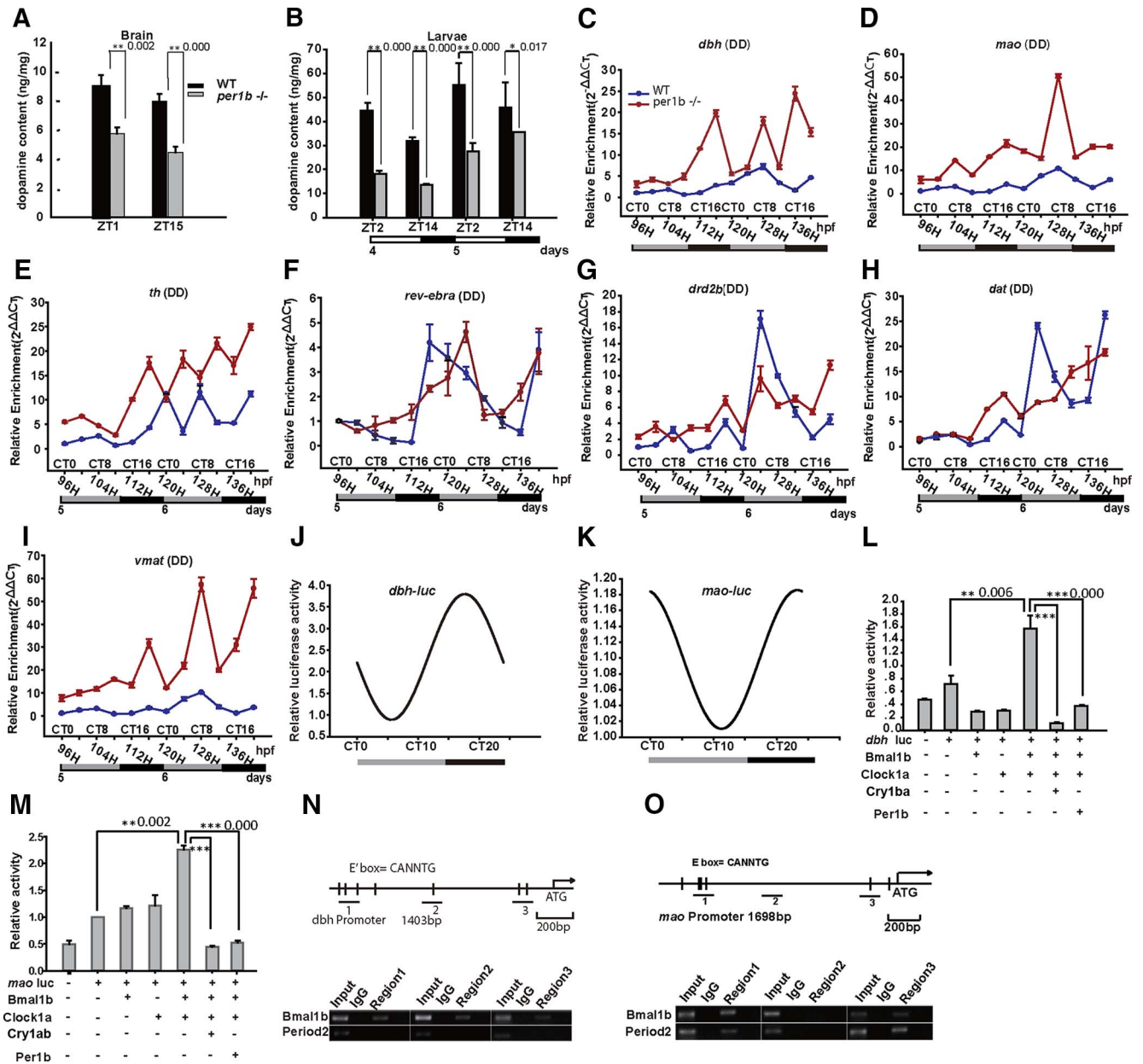
Figure 4. Circadian regulation of *dbh* and *mao* and impaired DA signaling in *per1b* mutant zebrafish. *A*, *B*, Reduced DA levels in the *per1b* mutant adult brain (*A*) and in larvae (*B*), determined by HPLC. These experiments were performed in triplicate, with three biological samples for each experiment. Data were analyzed using a one-way ANOVA test. All error bars are ±SEM. *C*, *D*, qRT-PCR showed rhythmic expression of *dbh* (*C*) and *mao* (*D*) in wild-type larvae and their upregulation in *per1b* mutants under DD conditions. One-way ANOVA test. *E*, Upregulation of *th* in the *per1b* mutant zebrafish. *F*, *rev-erbα* (*nr1d1*) shows a phase-delayed expression pattern in the *per1b* mutant fish under DD conditions. *G–I*, dopamine receptor D2 b (*drd2b*; *G*), dopamine transporter (*dat*; *H*), and vesicular monoamine transporter 2 (*vmat2*; *I*) in the *per1b* mutant zebrafish at most stages except for 124 hpf, when *drd2l* and *dat* were dramatically increased, which could be a response to the initiation of foraging at that stage (see text for detail). *J*, *K*, A continuous luminescence monitor assay with transgenic analysis showed rhythmic expression of *dbh* (*J*) and *mao* (*K*) in vivo. Data were normalized using CircleWave software. *L*, *M*, Cell transfection assays showed that *dbh* is activated by Clock1a and Bmal1b but repressed by Per1b or Cry1ba (*L*), while *mao* is activated by Clock1a and Bmal1b but repressed by Per1b or Cry1ab (*M*). Student's *t* test. *N*, *O*, ChIP assays showed that Bmal1b and Period2 proteins bind E′ boxes in the 5′ regulatory region of *dbh* (*N*) and *mao* (*O*). The top of *N* and *O* show the three fragments from the 5′ regulatory region of *dbh* for the ChIP assays. All the numbers on the right side of the star indicate the *p* values.

mimics an important symptom in psychiatric disorders, especially ADHD. Despite the difficulty to directly characterize the attention behavior of fish, the deficit in learning and memory of the *per1b* mutant fish could be easily extrapolated to be hyperactivity-derived "inattention."

per1b mutant fish display impulsivity-like phenotype

Human ADHD patients show impulsivity and often have difficulty waiting for things they want. To investigate whether zebrafish *per1b* mutants show cognitive impulsivity, we performed

a two-choice serial reaction-time task in adult fish as described previously (Parker et al., 2012), using a modified apparatus shown in Figure 1B. During 1-week-long consecutive daily training sessions, when a green light was accompanied by a food reward near the light, both the mutant and wild-type fish entered into the region near the green light within 1 min after it was switched on. In the following test phase, the green light was switched on but food was not added until a waiting period of 4 min. Results showed that during the 4 min waiting period, ~35% of wild-type fish maintained their attention to the task and stayed

near the green light at the first day of test, and the proportion of wild types remaining near the green light in the waiting period increased with subsequent trials. In contrast, only ~15% of *per1b* mutants stayed near the green light on the first test day, and although the proportion of fish remaining near the green light in the waiting period gradually increased in the following days as in wild types, this proportion was always significantly lower than that for wild types (Fig. 3G). Results are consistent with those displayed by rodent models of ADHD that were tested using a similar behavioral task (Bruno et al., 2007), indicating that *per1b* mutant fish display impulsivity. In addition, it is noteworthy that despite having learned the task, *per1b* mutants could not maintain their attention on the task at hand, as expected for an attention-deficit phenotype.

ADHD patients also tend to show impulsive behaviors, i.e., an inability to hold in check maladaptive behaviors. The persistent mirror-attacking behavior of the *per1b* mutant fish described above also can be construed as a trait similar to increased impulsivity or aggressiveness that makes the fish seemingly unable to break off ineffective behaviors (Fig. 3C; Movie 2).

Human patients who suffer from an impulsive control disorder frequently display an enhanced sense of arousal and are much more sensitive than other people to changes in the environment (Hollander and Stein, 2006). To test the response of *per1b* mutants to rapid change, we programed the ZebraLab aquarium system to deliver pulses of 90 s of light followed by 90 s of dark to the 96-well plate containing 6 dpf larvae. We used the distance larvae swam in 90 s to estimate the locomotor response to the rapid light/dark changes. Results showed that *per1b* mutants are much more sensitive to the quick light/dark changes and are noticeably more agitated during the dark pulse than their wild-type controls (Fig. 3H), mimicking the agitated state of human ADHD patients. These results show that *per1b* mutant fish clearly display hyperactivity, forgetfulness, and impulsivity, all ADHD-like behaviors, described in the *Diagnostic and Statistical Manual of Mental Disorders, Fifth Revised Edition* (*DSM-V*), by the American Psychiatric Association.

Disruption of the DA signaling pathway in *per1b* mutants

To elucidate the physiological basis for ADHD-like behaviors in *per1b* mutant zebrafish, we examined DA levels because an abnormal DA system has been implicated in the etiology and pathogenesis of ADHD (Gong et al., 2011; Lange et al., 2012). Results showed that whole larval bodies and adult brains of *per1b* mutants contained significantly lower levels of DA than wild-type controls (Fig. 4A,B; t test, $p < 0.05$) as assessed by HPLC. This result is consistent with findings for human ADHD patients and hypodopaminergic rodent models for ADHD (Gong et al., 2011). To investigate whether the circadian clock plays a role in regulating DA biosynthesis, metabolism, and signaling, we first examined expression of the *mao* gene, which encodes monoamine oxidases for decomposing DA into DOPAC. Results showed that *mao* is rhythmically expressed in wild-type larvae and upregu-
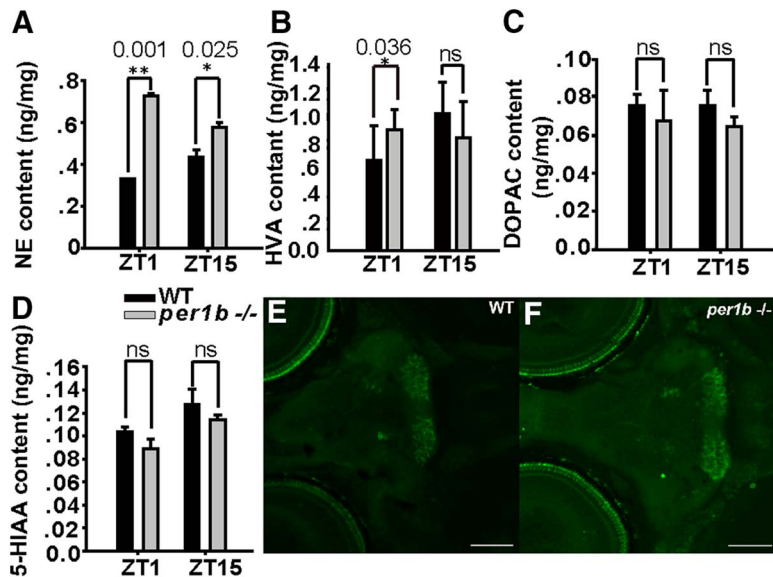
Figure 5. DA metabolites (HVA and DOPAC) and other catecholamines in *per1b* mutant and wild-type adult fish brains. *A*, NE is significantly increased in the *per1b* mutant brain both in the daytime (ZT1) and in the nighttime (ZT15). *B*, The DA metabolite HVA is increased in the *per1b* mutant brain only in the daytime (ZT). *C, D*, No significant changes of the DA metabolite DOPAC (*C*) and 5-HIAA (the terminal metabolite of brain serotonin) were apparent in the *per1b* mutant brain compared with wild types. Numbers on the right side of the star indicate *p* values. *E, F*, No significant changes of serotonin (5-hydroxytryptamine) neurons in the 6 dpf *per1b* mutant brain (*F*) compared with wild types (*E*). Scale bar, 100 μm.

lated in *per1b* mutant larvae (Fig. 4D). DA can also be converted into NE, catalyzed by DA β hydroxylase and we observed that *dbh* is rhythmically expressed and upregulated in *per1b* mutants (Fig. 4C). We also found that *th* (TH, ENS-DARG00000030621) was upregulated in *per1b* mutants (Fig. 4E), which may be a compensatory response to the high expression levels of *mao* and *dbh*. A recent study showed that mouse *Rev-erbα* (*Nr1d1*, ENSDARG00000030621) inhibits *Th* expression (Chung et al., 2014). Here we examined zebrafish *rev-erbα* expression and found that it oscillates in wild types but exhibits an ~8 h phase delay in mutants relative to wild types (Fig. 4F), likely resulting in a phase advance of *th* expression (Fig. 4E). In addition, *dat* (dopamine transporter, ENS-DARG00000004219), *drd2b* (dopamine receptor d2b, ENSDARG00000030621), and *vmat* (vesicular monoamine transporter, ENSDART00000025466) genes were all upregulated in *per1b* mutant larvae in all developmental stages except for 124 hpf, when *dat* and *drd2b* were dramatically increased in wild-type larvae (Fig. 4G–I). In *Caenorhabditis elegans*, DA is essential for sensing food and D1-like DA receptor DOP4 is responsible for this sensation (Ezcurra et al., 2011). Thus, it is likely that the increased expression of *dat* and *drd2b* at 124 hpf may correspond to the initiation of foraging in zebrafish larvae at that stage. The underlying mechanism, however, requires further investigation. Previous studies showed that juvenile and adult ADHD patients have increased levels of striatal DA transporter (Dougherty et al., 1999; Cheon et al., 2003), which may result in reduced synaptic DA. The DA D2/3 receptor is markedly upregulated in adolescent ADHD patients (Lou et al., 2004). Thus, high expression of *dat* and *drd2b* may also contribute to the ADHD-like phenotype in zebrafish. The vesicular monoamine transporter is responsible for the uptake of cytosolic monoamines into synaptic vesicles, and the increase of DA release through amphetamine treatment results in a significantly lower level of *vmat* expression (Glaser and Gerhardt, 2012). Thus, the observed
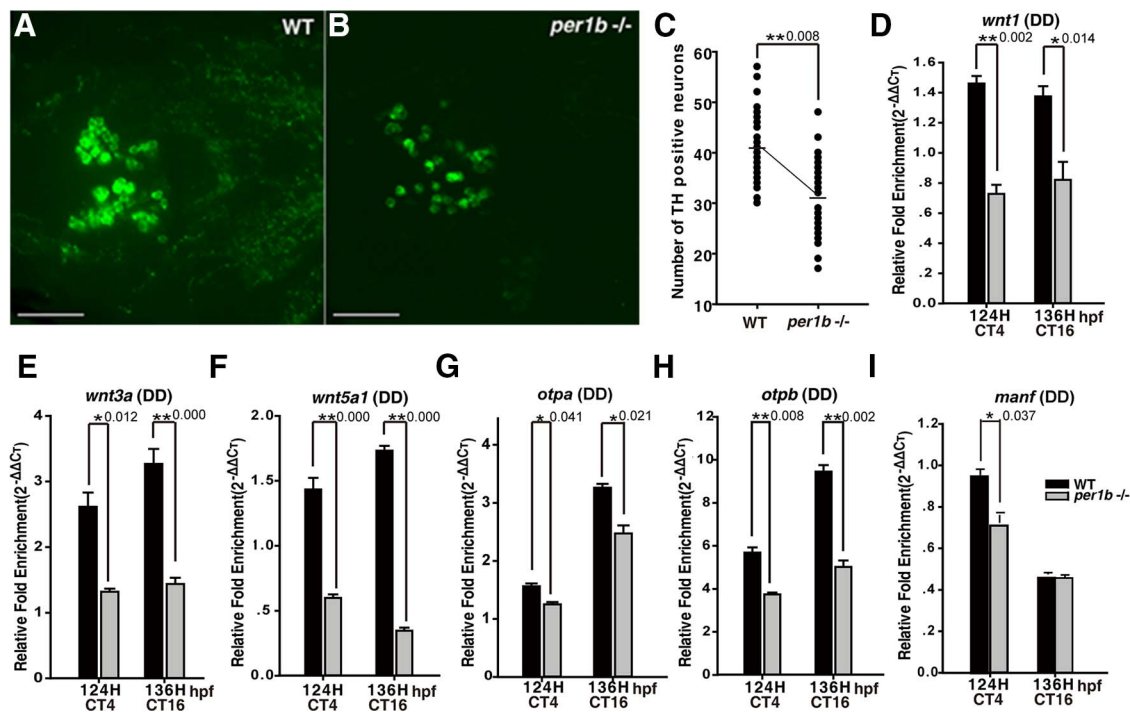
Figure 6. Partial loss and disorganization of dopaminergic neurons in the PT of the ventral diencephalon and downregulation of critical genes involved in specification, differentiation, and development or maintenance of dopaminergic neurons in *per1b* mutant zebrafish. ***A*, *B***, Dopaminergic neurons in the PT of the ventral diencephalon of 5 dpf larvae (anterior to left), stained by anti-TH antibody. Scale bar, 50 μm. ***C***, Numbers of positive TH neurons in *per1b* mutants and wild types, quantified with ImageJ cell counter function in double-blind scoring. Student's *t* test. ***D–I***, Downregulation of signaling proteins *wnt1* (***D***), *wnt3a* (***E***), and *wnt5a* (***F***) and of transcription factors *otpa* (***G***), *otpb* (***H***), and *manf* (***I***) involved in specification, differentiation, development, or maintenance of the dopaminergic neurons under DD conditions. Experiments were performed in triplicate, with three biological samples for each experiment. Data were analyzed using the Student's *t* test. All error bars are $\pm$SEM. Numbers on the right side of the star indicate *p* values.

upregulation of *vmat* also may be a compensatory response to the lower level of DA in *per1b* mutants.

The promoters of *dbh* and *mao* both harbor a specific *cis*-element, the E-like box (CANNTG), as do other clock-controlled genes (Vallone et al., 2004), suggesting the hypothesis that *dbh* and *mao* may be regulated by the circadian clock. To test this hypothesis, we placed *dbh* and *mao* promoter fragments containing E-like boxes into luciferase-based reporter constructs, microinjected them into one-cell zebrafish embryos, and generated stable transgenic zebrafish lines. Real-time monitoring showed that *dbh* and *mao* both oscillated *in vivo* (Fig. 4*J*,*K*). To see whether *dbh* and *mao* are controlled by the circadian system *in vitro*, we also performed cell-transfection assays using mammalian NIH3T3 cells and these luciferase constructs. Activities of *dbh* and *mao* promoters were significantly enhanced when cotransfected with Clock1a and Bmal1b (or Clock2 and Bmal1b for *mao*), but cotransfection of expression vectors for the negative regulators, Cry1ba (or Cry1ab for *mao*) or Per1b, markedly reduced the promoter activities in NIH3T3 cells (Fig. 4*L*,*M*).

To investigate whether *dbh* and *mao* genes are regulated by circadian clock genes *in vivo*, we performed ChIP experiments with a Bmal1b polyclonal antibody and a Period2 monoclonal antibody. Results showed that Bmal1b protein binds specifically to the E-like box elements of *dbh* and *mao* promoter regions, which may activate expression of the two genes, while Per2 just binds to the E-like boxes of *mao* (Fig. 4*N*,*O*). These results unambiguously showed that both *dbh* and *mao* are controlled directly by the circadian clock.

To determine whether the upregulation of *dbh* and *mao* transcription in the *per1b* mutant leads to higher enzymatic activities, we measured enzymatic products. We observed significantly in-

creased levels of NE (Fig. 5*A*) and HVA (Fig. 5*B*) in the *per1b* mutant, showing that upregulation of *dbh* and *mao* mRNA (Fig. 4*C*,*D*) results in more DA β hydroxylase and monoamine oxidase activity in *per1b* mutant fish. Because increased levels of NE were reported in both human ADHD patients and the mice ADHD model *coloboma* (Jones and Hess, 2003; Nestler et al., 2009), we think that elevated NE may also contribute to the behavioral phenotypes of *per1b* mutants; for instance, hypersensitive to rapid changes in light/dark periods and overagitation during the dark pulse (Fig. 3*G*), although the exact mechanism remains to be investigated. The levels, however, of both 5-HIAA (the final metabolite of brain serotonin; Fig. 5*D*) and serotonin neurons (Fig. 5*E*,*F*) are normal in *per1b* mutant fish, implying that serotonin (5-hydroxytryptamine) is not affected in *per1b* mutant fish.

Altered dopaminergic neuron development in *per1b* mutants

In mammals, dopaminergic neurons in the ventral tegmental area of the midbrain and in the substantia nigra compacta (VTA/SNc) regulate complex behaviors, such as cognition, motivation, learning, and motor activity (Luo et al., 2011). In zebrafish, dopaminergic neurons in the PT of the ventral diencephalon, which project into the subpallium, have been likewise implicated in the regulation of complex behaviors (Tay et al., 2011). The seven distinct populations of dopaminergic neurons in the zebrafish PT integrate ascending and descending circuits for control of locomotion (Rink and Wullimann, 2002). Very little is known, however, concerning the possible effects of the development of these zebrafish dopaminergic neurons on the pathogenesis of ADHD (Lange et al., 2012). With double-blind scoring, we observed a significant decrease in the number of dopaminergic neurons in the *per1b* mutant ventral diencephalic PT at 5 dpf in comparison
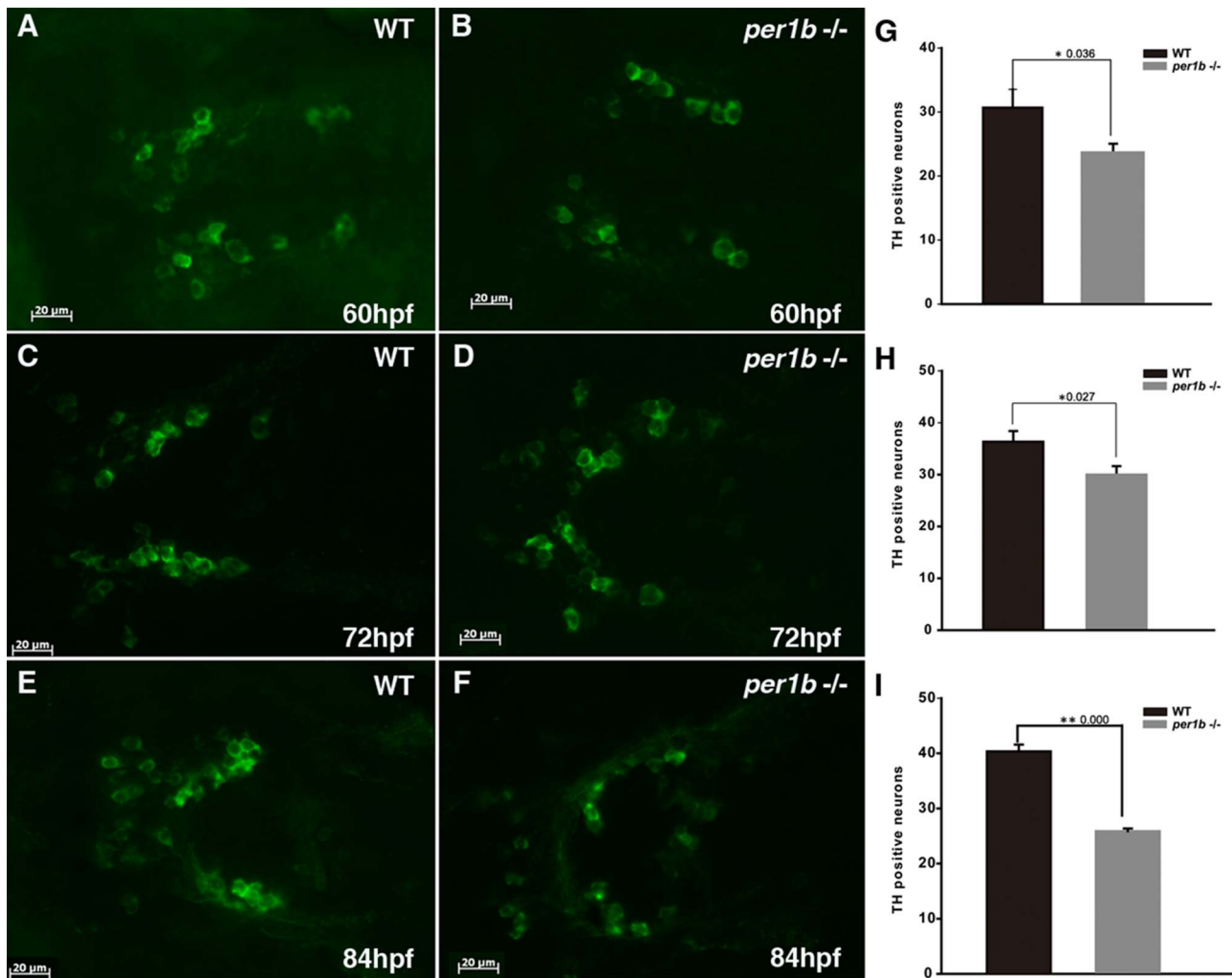
Figure 7. Continual loss of dopaminergic neurons in the PT of the ventral diencephalon from 60 – 84 hpf in *per1b* mutant zebrafish. *A*, *C*, *E*, Dopaminergic neurons in the wild-type PT. *B*, *D*, *F*, Dopaminergic neurons in the *per1b* mutant PT. Scale bar, 20 μm. *G–I*, The numbers of dopaminergic neurons in wild-type and *per1b* mutant larvae, determined with ImageJ in a double-blind manner. $n = 12$. Data were calculated in three independent experiments. Student's *t* test was used in the statistical analysis. Error bars are ±SEM. Numbers on the right side of the star indicate *p* values.

with wild-type controls (Fig. 6A–C). Deficit of dopaminergic neurons occurred as early as 60 – 84 hpf and continued thereafter in *per1b* mutants (Fig. 7). In addition, dopaminergic neurons in the *per1b* mutant PT appeared to be sparsely distributed and disorganized, rather than forming the regular seven populations as in the wild-type PT (Fig. 6A,B). This result shows that *per1b* activity is required for normal development or patterning of dopaminergic neurons.

To investigate possible mechanisms underlying the reduction and disorganization of dopaminergic neurons in the *per1b* mutant PT, we examined the expression of genes that play roles in specification, differentiation, and development or maintenance of dopaminergic neurons. In these experiments, only DD conditions were used to examine circadian regulation of these genes. Both orthopedia homeodomain protein (Otp) a (ENSDARG00000014201) and Otpb (ENSDARG00000058379) are required for the specification and development of dopaminergic neurons (Ryu et al., 2007); Wnt factors are critical for dopaminergic neuron differentiation and axonal extension (Castelo-Branco et al., 2003); and mesencephalic astrocyte-derived neurotrophic factor (Manf) plays a pivotal role in protecting dopaminergic neurons from neurotoxic damage (Chen et al., 2012). RT-PCR showed that *wnt1* (ENSDARG00000055554), *wnt3a* (ENSDARG00000058822),

wnt5a (ENSDARG00000014495; Fig. 6D–F), *otpa*, *otpb* (Fig. 6G,H), and *mesencephalic astrocyte derived neurotrophic factor* (*manf*, NM_001076629; Fig. 6I) are all significantly downregulated in *per1b* mutants under DD conditions. These results suggest that Per1b acts via Otp, Wnt signaling, and Manf to regulate specification, differentiation, development, and maintenance of dopaminergic neurons, but the mechanisms by which Per1b regulates these genes require further investigation. In addition, *LATROPHILIN3* (*LPHN3*), which encodes a putative adhesion-G-protein-coupled receptor, has recently been implicated as an ADHD-susceptible gene (Arcos-Burgos et al., 2010). Knockdown of *lphn3.1*, a zebrafish ortholog of *LPHN3*, results in reduction and misplacement of dopaminergic neurons in the ventral diencephalic PT and a hyperactive/impulsive phenotype (Lange et al., 2012). Consistent with those findings, we observed that *lphn3.1* is significantly downregulated in *per1b* mutants (see Fig. 9A).

Per1 knock-out mice display ADHD behaviors and reduced levels of DA

To confirm the broad phylogenetic significance of our findings, we examined *Per1* knock-out mice (Bae et al., 2001; strain name: B6.129-*Per1*[tm1Drw]/J, http://jaxmice.jax.org/strain/010491.html) to see whether disruption of the circadian clock results in ADHD
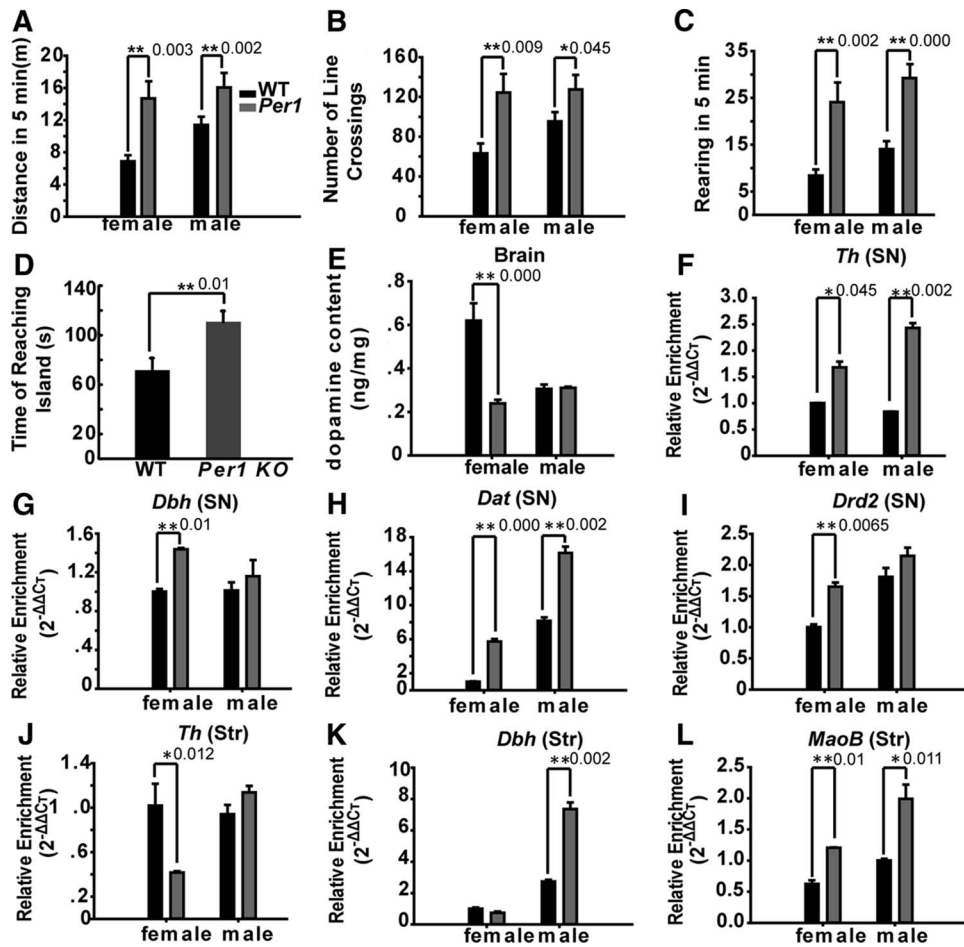
Figure 8. *Per1* knock-out mice display ADHD-like symptoms, lower levels of DA, and abnormal expression of DA metabolism and signaling transduction pathway genes. *A*, Distances that wild-type mice and *Per1* knock-out mice (*n* = 12 each) traveled in 5 min. *B*, Lines crossed in an open-field test during 5 min. *C*, The average rearing frequency during 5 min tests. Wild-type mice, *n* = 12; *Per1* knock-out mice. *n* = 12. Three sets of tests for each animal. *D*, The learning and memory abilities of wild-type mice and *Per1* knock-out mice. *n* = 12. Data were calculated for three independent experiments. *E*, The DA level decreased in the brain of *Per1* knock-out female mice compared with wild-type mice. Experiments were performed in triplicate, with three biological samples for each experiment. Data were analyzed using Student's *t* test. All error bars are ±SEM. *F–I*, *Th* (*F*), *Dbh* (*G*), *Dat* (*H*), and *Drd2* (*I*) are significantly upregulated in the SN of *Per1* knock-out mice midbrain. *J*, The *Th* expression level is downregulated in the corpus striatum (Str) region of *Per1* knock-out mice. *K*, *L*, *Dbh* (*K*) and *MaoB* (*L*) are upregulated in the striatum region of *Per1* knock-out mice. Numbers on the right side of the star indicate *p* values.

symptoms in mammals as it does in fish. Using an open-field apparatus, we found that *Per1* knock-out mice were hyperactive and impulsive (Fig. 8A–C) estimated by running distance and rearing frequency, respectively, and by the water maze assay, we observed that *Per1* knock-out mice displayed impaired learning and memory (Fig. 8D). We also found that the DA level in the *Per1* knock-out female mouse brain was significantly lower than in wild-type controls, as in zebrafish (Fig. 8E). We also examined the expression levels of genes involved in DA metabolism and signaling transduction pathways by qRT-PCR in the VTA/SNc. As in zebrafish *per1b* mutants, genes involved in DA metabolism and signal transduction were disregulated in *Per1* knock-out mice either in the SN or corpus striatum (Fig. 8F–L). Although *Per1* knock-out male mice also displayed ADHD-like symptoms and altered DA-related genes, we did not detect significantly lower levels of DA in their brains, which requires further investigation. Thus, it appears that circadian regulation of ADHD pathogenesis is highly conserved among vertebrate species.

Hyperactivity and impulsivity of *per1b* mutants can be rescued by ADHD drugs
If *per1b* mutant zebrafish mimic ADHD, then they should respond to drugs used to treat ADHD patients. ADHD thera-

peutic agents include deprenyl (Selegiline), a monoamine oxidase inhibitor, and methylphenidate (MPH, or Ritalin), an amphetamine-like compound that represses DA transporter. These drugs can temporally restore extracellular DA levels and thus relieve some ADHD symptoms, including hyperactivity (Zhu et al., 2014). We treated larvae with different concentrations of MPH or deprenyl by directly adding the drug to the water for 1 h and then measured mean swimming speed. We found that treatment with 5 μM of either MPH or deprenyl was sufficient to reduce the hyperactivity of *per1b* mutant larvae to approximately the activity level of wild-type controls, but that the same concentration of these drugs exerted no effect on locomotion of wild-type larvae (Fig. 9B,C). These results show that, as in human ADHD patients and rodent models of ADHD, treatment with Ritalin or Selegiline was sufficient to rescue hyperactivity in the *per1b* mutant larvae.

Because these drugs also help reduce impulsive actions and improve attention and cognition (Geissler and Lesch, 2011), we tested whether Ritalin can rescue the mirror-attacking phenotype of *per1b* mutant zebrafish. The persistent mirror-attacking behavior of *per1b* mutant adult fish was significantly reversed with a 1 h treatment of 100 μM Ritalin (Fig. 9D; Movie 2). While we regard the mirror-attacking phenotype of *per1b* mutant fish as impulsive or aggressive behavior, it also
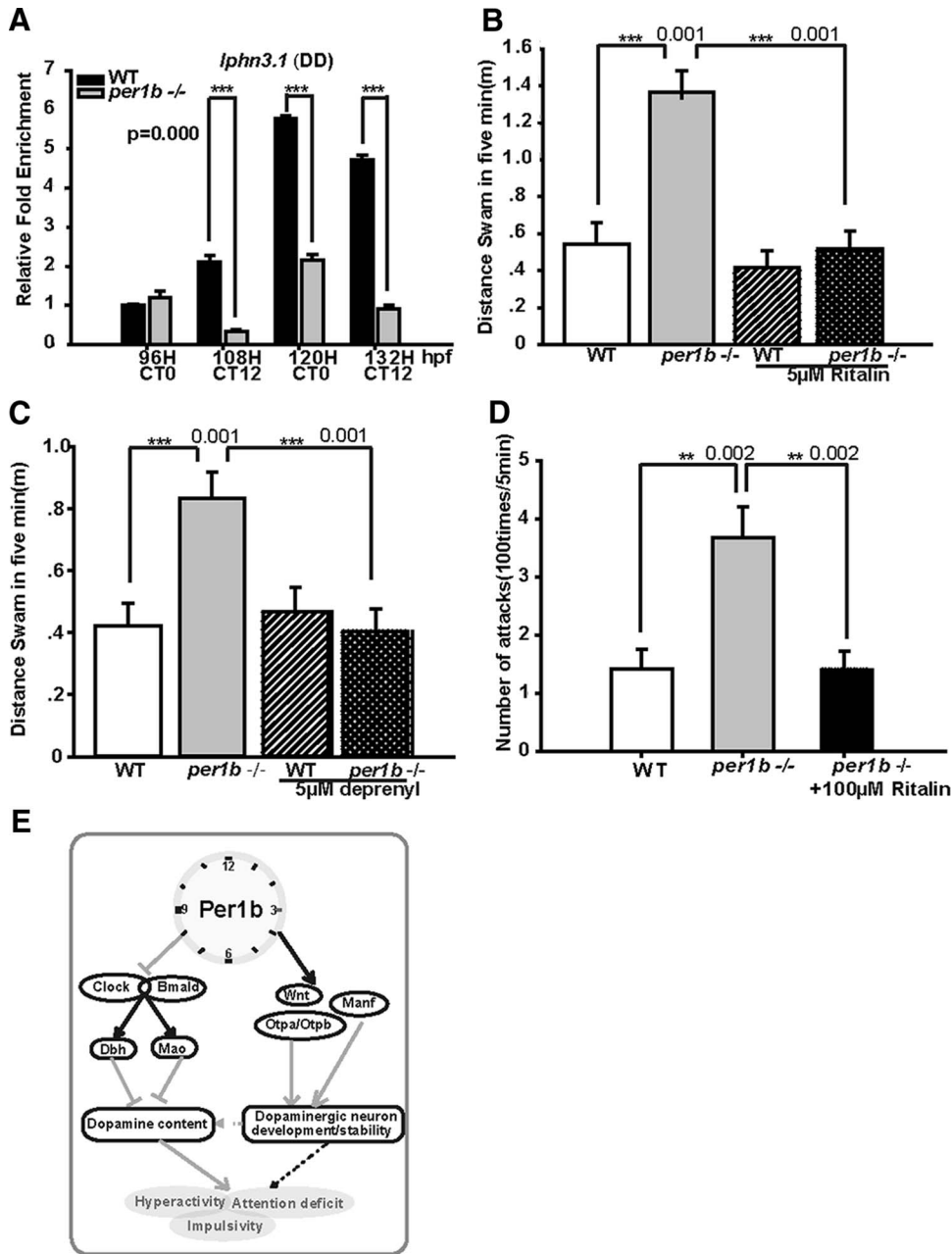
Figure 9. Rescue experiments with ADHD treatment drugs MPH (Ritalin) and deprenyl (Selegiline) and a model for the regulatory roles of Per1b in ADHD. *A*, downregulation of the ADHD-susceptible gene *lphn3.1* (*latrophilin 3.1*) in *per1b* mutant zebrafish as shown by qRT-PCR. Error bars are ±SEM. Student's *t* test. *B*, Rescue of *per1b* mutant hyperactivity by MPH treatment. Shown are swimming distances in 5 min intervals of 6 dpf MPH-treated and control larvae. Wild-type (*n* = 18) and *per1b* mutant larvae (*n* = 18) before and after a 1 h treatment with 5 μM MPH. The same larvae were analyzed before and after treatment. Student's *t* test. *C*, Rescue of *per1b* mutant hyperactivity by deprenyl treatment. Shown are swimming distances in 5 min intervals of 6 dpf deprenyl-treated and control larvae. Wild-type (*n* = 18) and *per1b* mutant larvae (*n* = 18) before and after a 1 h treatment with 5 μM deprenyl. Student's *t* test. *D*, Rescue of *per1b* mutant impulsivity by MPH treatment. Shown are mirror-attack times in 5 min intervals of 3-month-old MPH-treated and control adult fish. Wild-type (*n* = 18) and *per1b* mutant fish (*n* = 18) before and after a 1 h treatment with 100 μM MPH. The same fish were analyzed before and after treatment. Student's *t* test (Movie 2). *E*, A model for the role of Per1b in ADHD through regulation of DA metabolism/degradation and dopaminergic neuron development and maintenance. The circadian clock regulates *mao* and *dbh*. Additionally, Per1b itself or the circadian clock system directly or indirectly acts via *otpa*, *otpb*, *wnts*, and *manf*, which are critical for specification, differentiation, development, and maintenance of dopaminergic neurons. The purpose of this action is probably regulate the number and organization of dopaminergic neurons in the ventral diencephalic PT. Numbers on the right side of the star indicate *p* values.

mimics hyperactivity or perseveration of ADHD (*DSM-V*). The observation that ADHD drugs can rescue both the hyperactivity and mirror-attacking phenotypes of *per1b* mutant fish supports our notion that this circadian mutant zebrafish is an invaluable tool for investigation of ADHD pathogenesis and serves to identify other drugs that might be useful for human patients.

Discussion

We have established a mutant with altered circadian rhythms that clearly displays hyperactive, defective learning and memory, and impulsivity-like symptoms. These findings lead us to propose that these phenotypes mimic the symptoms of human ADHD patients and that *per1b* mutant fish should be used for studying

Table 1. Comparisons between human ADHD and some animal models for ADHD

Subject	Modification	Hyperactivity	Rescued by therapeutic treatments		Impulsivity	Inattentiveness	DA level	Disrupted dopaminergic neuron
			Ritalin (MPD)	Seleginine (deprenyl)				
ADHD (human)		Yes (Geissler and Lesch, 2011)	Yes (Geissler and Lesch, 2011)	Yes (Akhondzadeh et al., 2003)	Yes (Pastor et al., 2008)	Yes (Pastor et al., 2008)	Decrease	Not determined
Guanylyl cyclase-c (*Gc-c*) knock-out (mouse)	Knock-out of the *Gc-c* gene	Yes (Gong et al., 2011)	Yes (Gong et al., 2011)	Not determined	Yes (Gong et al., 2011)	Yes (Gong et al., 2011)	Decrease (Gong et al., 2011)	Not determined
Coloboma mutant (mouse)	Mutation on the *SNAP-25* gene	Yes (Hess et al., 1992)	No (Hess et al., 1996)	Not determined	Yes (Bruno et al., 2007)	Not determined	Not determined	Not determined
per1b mutant (zebrafish)	Retrovirus insertion in the *per1b* gene	Yes	Yes	Yes	Yes	Yes	Decrease	Yes
Per1 knock-out (mouse)	Knock-out of the *Per1* gene	Yes	Not determined	Not determined	Yes	Yes	Decrease	Not determined

the mechanistic basis of ADHD (Fig. 9E; Table 1). Like human ADHD patients and rodent models of ADHD (Gong et al., 2011), homozygous *per1b* mutant zebrafish display hyperactivity, impulsiveness, and impairment of sustained attention (Fig. 3A–H); contain low levels of DA; and respond to the ADHD treatment drugs Ritalin (MPH) and Seleginine (deprenyl) (Fig. 9B–D; Table 1). These results demonstrate not only that *per1b* mutant zebrafish meet the criteria of face validity, construct validity, and predictive validity of ADHD models, but also that a dysfunctional DA system is a highly conserved hallmark of ADHD in human, rodents, and zebrafish (Gong et al., 2011; Baird et al., 2012; Lange et al., 2012; Table 1). Furthermore, we also observed that *Per1* knock-out mice display ADHD-like symptoms, suggesting that circadian roles in ADHD pathogenesis are highly conserved (Fig. 8E). Although we were unable to detect any protein signal in the DA neurons, likely due to the suboptimal zebrafish Per1b antibody, the RNA *in situ* hybridization results showed that *per1b* is ubiquitously expressed in the brain (Fig. 2E). Our assumption that *per1b* is expressed in the PT region is also based on our antibody-staining result of TH and PER1 colocalization in the SN/VTA DA neurons in mice (Fig. 2H). Even though zebrafish Per1b is not expressed in the PT region, it may still play an indirect role in the PT region.

Recent GWAS suggest that ADHD is polygenic (Franke et al., 2012), and implicate circadian genes, particularly *PER1*, as possible ADHD-susceptible genes (Lasky-Su et al., 2008; Xu et al., 2010). First of all, our work shows how zebrafish research can be useful for evaluating human GWAS. For example, we show that among single nucleotide polymorphism in the human *PER1* locus is among the many genes associated with ADHD, along with many other genes (Lasky-Su et al., 2008). In addition, however, our work shows a causative relationship and provides a mechanism for the association.

Previous studies have already revealed that canonical circadian clock genes play important roles in cognitive and psychiatric behaviors (Karatsoreos, 2014). For instance, both *Bmal1* and *Period2* knock-out mice display mania-like behavior (McClung, 2013), while *Cry1* and *Cry2* double-knock-out mice exhibit cognitive dysfunction and elevated anxiety (De Bundel et al., 2013). In particular, both *Clock* and *Rev-erbα* can regulate TH, the rate-limiting enzyme in the biosynthesis of DA and other catecholamines, and mice lacking either *Clock* or *Rev-erbα* display elevated midbrain dopaminergic activities and mania-like behavior (Roybal et al., 2007; Chung et al., 2014). Here, our study found that the circadian clock directly controls *mao* and *dbh*, which are involved in DA catabolism and the conversion of DA into NE, respectively. Transcription of these two genes are activated by the Clock:Bmal heterodimer but repressed by Per1b, and loss of Per1b function leads to *mao* and *dbh* upregulation, which may in turn result in DA reduction and thus contribute to ADHD (Fig. 9E). While the circadian control of *MaoA* (an ortholog of zebrafish *mao*) transcription was reported previously in mouse (Hampp et al., 2008), our study is the first to show direct regulation of *dbh* by the circadian clock.

Even though ADHD has long been regarded as a neurodevelopmental disorder, the underlying mechanism remains largely unknown (Lange et al., 2012). Our study suggests a mechanism for the impaired development of dopaminergic neurons in ADHD, as well as regulatory roles of Per1b on genes essential for development or maintenance of dopaminergic neurons. In zebrafish *per1b* mutants, *otpa*, *otpb*, *wnt1*, *wnt3a*, *wnt5a*, and *manf*, which are critical for specification, differentiation, development, or maintenance of dopaminergic neurons, were all downregulated. Downregulation of these genes could lead to the observed partial loss and disorganization of dopaminergic neurons in the *per1b* mutant diencephalic PT. Impairment of dopaminergic neuron development also should lead to DA reduction and ADHD-like symptoms (Fig. 9E).

In summary, Per1b is required to prevent ADHD-like symptoms in zebrafish and appears to work by regulating endogenous DA levels in two ways (Fig. 9E): first, by acting through DA-related enzymes, transporters, and receptors to directly regulate the endogenous DA level, and second, by acting through genes critical for specification, differentiation, development, or maintenance of dopaminergic neurons to possibly regulate the number and spatial organization of dopaminergic neurons (Fig. 9E). Zebrafish possesses two orthologs of the mammalian *Per1* gene, *per1a* and *per1b*. These were derived from the teleost genome duplication, which occurred ~300 million years ago (Amores et al., 1998; Postlethwait and Braasch, 2012). The role of Per1a in ADHD remains to be investigated. However, our previous study showed that *per1a* has a rather more specific expression pattern than *per1b*, and has evolved distinct molecular mechanisms underlying temporal and spatial expression (Wang, 2008), which suggests that *per1a* either plays a compensatory role for *per1b* or has a different function from *per1b*. Nevertheless, our *per1b* mutant provides not only new insights into the pathogenesis of ADHD, but importantly, identifies *Per1* as a new therapeutic tar-

get for ADHD diagnosis and treatment. Unlike many rodent models for ADHD (Yamada, 2011), *per1b* mutant zebrafish have normal body weight and body length, and show no signs of obvious physiological or metabolic defects. The fact that *per1b* mutant fish contain lower levels of DA than wild types makes them a particularly good subject for studying mechanisms underlying hypodopaminergic ADHD and behaviors. Because zebrafish are readily suitable for large-scale and high-throughput drug discovery (Lieschke and Currie, 2007), this zebrafish *per1b* mutant should be invaluable in identifying new drugs for potential treatments of the neuropsychiatric disorders associated with the alteration of the brain dopaminergic system, such as ADHD, Parkinson's disease, and addiction (Hollander and Stein, 2006).

References

Akhondzadeh S, Tavakolian R, Davari-Ashtiani R, Arabgol F, Amini H (2003) Selegiline in the treatment of attention deficit hyperactivity disorder in children: a double blind and randomized trial. Prog Neuropsychopharmacol Biol Psychiatry 27:841–845. CrossRef Medline

Alsop B (2007) Problems with spontaneously hypertensive rats (SHR) as a model of attention-deficit/hyperactivity disorder (AD/HD). J Neurosci Methods 162:42–48. CrossRef Medline

Amores A, Force A, Yan YL, Joly L, Amemiya C, Fritz A, Ho RK, Langeland J, Prince V, Wang YL, Westerfield M, Ekker M, Postlethwait JH (1998) Zebrafish hox clusters and vertebrate genome evolution. Science 282: 1711–1714. CrossRef Medline

Appelbaum L, Wang G, Yokogawa T, Skariah GM, Smith SJ, Mourrain P, Mignot E (2010) Circadian and homeostatic regulation of structural synaptic plasticity in hypocretin neurons. Neuron 68:87–98. CrossRef Medline

Arcos-Burgos M, Jain M, Acosta MT, Shively S, Stanescu H, Wallis D, Domené S, Vélez JI, Karkera JD, Balog J, Berg K, Kleta R, Gahl WA, Roessler E, Long R, Lie J, Pineda D, Londoño AC, Palacio JD, Arbelaez A, et al. (2010) A common variant of the latrophilin 3 gene, LPHN3, confers susceptibility to ADHD and predicts effectiveness of stimulant medication. Mol Psychiatry 15:1053–1066. CrossRef Medline

Bae K, Jin X, Maywood ES, Hastings MH, Reppert SM, Weaver DR (2001) Differential functions of mPer1, mPer2, and mPer3 in the SCN circadian clock. Neuron 30:525–536. CrossRef Medline

Baird AL, Coogan AN, Siddiqui A, Donev RM, Thome J (2012) Adult attention-deficit hyperactivity disorder is associated with alterations in circadian rhythms at the behavioural, endocrine and molecular levels. Mol Psychiatry 17:988–995. CrossRef Medline

Ben-Moshe Z, Alon S, Mracek P, Faigenbloom L, Tovin A, Vatine GD, Eisenberg E, Foulkes NS, Gothilf Y (2014) The light-induced transcriptome of the zebrafish pineal gland reveals complex regulation of the circadian clockwork by light. Nucleic Acids Res 42:3750–3767. CrossRef Medline

Bolyard KJ, Rowland WJ (1996) Context-dependent response to red coloration in stickleback. Anim Behav 52:5.

Bruno KJ, Freet CS, Twining RC, Egami K, Grigson PS, Hess EJ (2007) Abnormal latent inhibition and impulsivity in coloboma mice, a model of ADHD. Neurobiol Dis 25:206–216. CrossRef Medline

Castelo-Branco G, Wagner J, Rodriguez FJ, Kele J, Sousa K, Rawal N, Pasolli HA, Fuchs E, Kitajewski J, Arenas E (2003) Differential regulation of midbrain dopaminergic neuron development by Wnt-1, Wnt-3a, and Wnt-5a. Proc Natl Acad Sci U S A 100:12747–12752. CrossRef Medline

Cermakian N, Monaco L, Pando MP, Dierich A, Sassone-Corsi P (2001) Altered behavioral rhythms and clock gene expression in mice with a targeted mutation in the Period1 gene. EMBO J 20:3967–3974. CrossRef Medline

Chen YC, Sundvik M, Rozov S, Priyadarshini M, Panula P (2012) MANF regulates dopaminergic neuron development in larval zebrafish. Dev Biol 370:237–249. CrossRef Medline

Cheon KA, Ryu YH, Kim YK, Namkoong K, Kim CH, Lee JD (2003) Dopamine transporter density in the basal ganglia assessed with [123I]IPT SPET in children with attention deficit hyperactivity disorder. Eur J Nucl Med Mol Imaging 30:306–311. CrossRef Medline

Cho H, Zhao X, Hatori M, Yu RT, Barish GD, Lam MT, Chong LW, DiTacchio L, Atkins AR, Glass CK, Liddle C, Auwerx J, Downes M, Panda S, Evans RM (2012) Regulation of circadian behaviour and metabolism by

REV-ERB-alpha and REV-ERB-beta. Nature 485:123–127. CrossRef Medline

Chung S, Lee EJ, Yun S, Choe HK, Park SB, Son HJ, Kim KS, Dluzen DE, Lee I, Hwang O, Son GH, Kim K (2014) Impact of circadian nuclear receptor REV-ERBalpha on midbrain dopamine production and mood regulation. Cell 157:858–868. CrossRef Medline

De Bundel D, Gangarossa G, Biever A, Bonnefont X, Valjent E (2013) Cognitive dysfunction, elevated anxiety, and reduced cocaine response in circadian clock-deficient cryptochrome knockout mice. Front Behav Neurosci 7:152. CrossRef Medline

Dijk DJ, von Schantz M (2005) Timing and consolidation of human sleep, wakefulness, and performance by a symphony of oscillators. J Biol Rhythms 20:279–290. CrossRef Medline

Dougherty DD, Bonab AA, Spencer TJ, Rauch SL, Madras BK, Fischman AJ (1999) Dopamine transporter density in patients with attention deficit hyperactivity disorder. Lancet 354:2132–2133. CrossRef Medline

Ezcurra M, Tanizawa Y, Swoboda P, Schafer WR (2011) Food sensitizes C. elegans avoidance behaviours through acute dopamine signalling. EMBO J 30:1110–1122. CrossRef Medline

Franke B, Faraone SV, Asherson P, Buitelaar J, Bau CH, Ramos-Quiroga JA, Mick E, Grevet EH, Johansson S, Haavik J, Lesch KP, Cormand B, Reif A, Reif A (2012) The genetics of attention deficit/hyperactivity disorder in adults, a review. Mol Psychiatry 17:960–987. CrossRef Medline

Geissler J, Lesch KP (2011) A lifetime of attention-deficit/hyperactivity disorder: diagnostic challenges, treatment and neurobiological mechanisms. Expert Rev Neurother 11:1467–1484. CrossRef Medline

Glaser PEA, Gerhardt GA (2012) The neuropsychopharmacology of stimulants: dopamine and ADHD. In: current directions in ADHD and its treatment (Norvilitis JM, ed). Rijeka, Croatia: InTech.

Golling G, Amsterdam A, Sun Z, Antonelli M, Maldonado E, Chen W, Burgess S, Haldi M, Artzt K, Farrington S, Lin SY, Nissen RM, Hopkins N (2002) Insertional mutagenesis in zebrafish rapidly identifies genes essential for early vertebrate development. Nat Genet 31:135–140. CrossRef Medline

Gong R, Ding C, Hu J, Lu Y, Liu F, Mann E, Xu F, Cohen MB, Luo M (2011) Role for the membrane receptor guanylyl cyclase-C in attention deficiency and hyperactive behavior. Science 333:1642–1646. CrossRef Medline

Gunn RK, Huentelman MJ, Brown RE (2011) Are Sema5a mutant mice a good model of autism? A behavioral analysis of sensory systems, emotionality and cognition. Behav Brain Res 225:142–150. CrossRef Medline

Hampp G, Ripperger JA, Houben T, Schmutz I, Blex C, Perreau-Lenz S, Brunk I, Spanagel R, Ahnert-Hilger G, Meijer JH, Albrecht U (2008) Regulation of monoamine oxidase A by circadian-clock components implies clock influence on mood. Curr Biol 18:678–683. CrossRef Medline

Harbers K, Kuehn M, Delius H, Jaenisch R (1984) Insertion of retrovirus into the first intron of alpha 1(I) collagen gene to embryonic lethal mutation in mice. Proc Natl Acad Sci U S A 81:1504–1508. CrossRef Medline

Hess EJ, Jinnah HA, Kozak CA, Wilson MC (1992) Spontaneous locomotor hyperactivity in a mouse mutant with a deletion including the Snap gene on chromosome 2. J Neurosci 12:2865–2874. Medline

Hess EJ, Collins KA, Wilson MC (1996) Mouse model of hyperkinesis implicates SNAP-25 in behavioral regulation. J Neurosci 16:3104–3111. Medline

Hollander E, Stein DJ (2006) Clinical manual of impulse-control disorders, 1st Edition. Arlington, VA: American Psychiatric Publishing.

Howard GC, Kaser MR (2007) Making and using antibodies: a practical handbook. Boca Raton, FL: CRC/Taylor and Francis.

Hurd MW, Debruyne J, Straume M, Cahill GM (1998) Circadian rhythms of locomotor activity in zebrafish. Physiol Behav 65:465–472. CrossRef Medline

Jones MD, Hess EJ (2003) Norepinephrine regulates locomotor hyperactivity in the mouse mutant coloboma. Pharmacol Biochem Behav 75:209–216. CrossRef Medline

Karatsoreos IN (2014) Links between circadian rhythms and psychiatric disease. Front Behav Neurosci 8:162. CrossRef Medline

Kendall T, Taylor E, Perez A, Taylor C, Guideline Development G (2008) Diagnosis and management of attention-deficit/hyperactivity disorder in children, young people, and adults: summary of NICE guidance. BMJ 337:a1239. CrossRef Medline

Kobayashi Y, Ishikawa T, Hirayama J, Daiyasu H, Kanai S, Toh H, Fukuda I, Tsujimura T, Terada N, Kamei Y, Yuba S, Iwai S, Todo T (2000) Molec-

ular analysis of zebrafish photolyase/cryptochrome family: two types of cryptochromes present in zebrafish. Genes Cells 5:725–738. CrossRef Medline

Lange M, Norton W, Coolen M, Chaminade M, Merker S, Proft F, Schmitt A, Vernier P, Lesch KP, Bally-Cuif L (2012) The ADHD-susceptibility gene lphn3.1 modulates dopaminergic neuron formation and locomotor activity during zebrafish development. Mol Psychiatry 17:946–954. CrossRef Medline

Lasky-Su J, Neale BM, Franke B, Anney RJ, Zhou K, Maller JB, Vasquez AA, Chen W, Asherson P, Buitelaar J, Banaschewski T, Ebstein R, Gill M, Miranda A, Mulas F, Oades RD, Roeyers H, Rothenberger A, Sergeant J, Sonuga-Barke E, et al. (2008) Genome-wide association scan of quantitative traits for attention deficit hyperactivity disorder identifies novel associations and confirms candidate gene associations. Am J Med Genet B Neuropsychiatr Genet 147B:1345–1354. CrossRef Medline

Lieschke GJ, Currie PD (2007) Animal models of human disease: zebrafish swim into view. Nat Rev Genet 8:353–367. CrossRef Medline

Liu Z, Huang M, Wu X, Shi G, Xing L, Dong Z, Qu Z, Yan J, Yang L, Panda S, Xu Y (2014) PER1 phosphorylation specifies feeding rhythm in mice. Cell Rep 7:1509–1520. CrossRef Medline

Lou HC, Rosa P, Pryds O, Karrebaek H, Lunding J, Cumming P, Gjedde A (2004) ADHD: increased dopamine receptor availability linked to attention deficit and low neonatal cerebral blood flow. Dev Med Child Neurol 46:179–183. Medline

Luo AH, Tahsili-Fahadan P, Wise RA, Lupica CR, Aston-Jones G (2011) Linking context with reward: a functional circuit from hippocampal CA3 to ventral tegmental area. Science 333:353–357. CrossRef Medline

McClung CA (2013) How might circadian rhythms control mood? Let me count the ways. Biol Psychiatry 74:242–249. CrossRef Medline

McClung CA, Sidiropoulou K, Vitaterna M, Takahashi JS, White FJ, Cooper DC, Nestler EJ (2005) Regulation of dopaminergic transmission and cocaine reward by the Clock gene. Proc Natl Acad Sci U S A 102:9377–9381. CrossRef Medline

Nestler EJ, Hyman SE, Malenka RC (2009) Molecular neuropharmacology: a foundation for clinical neuroscience, 2nd edition. New York: McGraw-Hill Medical.

Parker MO, Millington ME, Combe FJ, Brennan CH (2012) Development and implementation of a three-choice serial reaction time task for zebrafish (Danio rerio). Behav Brain Res 227:73–80. CrossRef Medline

Pastor PN, Reuben CA, National Health Interview Survey (U.S.), National Center for Health Statistics (U.S.) (2008) Diagnosed attention deficit hyperactivity disorder and learning disability, United States, 2004–2006: data from the National Health Interview Survey. Hyattsville, MD: U.S. Dept. of Health and Human Services, Centers for Disease Control and Prevention, National Center for Health Statistics.

Pendergast JS, Niswender KD, Yamazaki S (2012) Tissue-specific function of Period3 in circadian rhythmicity. PLoS One 7:e30254. CrossRef Medline

Philipsen A, Hornyak M, Riemann D (2006) Sleep and sleep disorders in adults with attention deficit/hyperactivity disorder. Sleep Med Rev 10: 399–405. CrossRef Medline

Postlethwait JH, Braasch I (2012) Polyploidy in fish and the teleost genome duplication. In: Polyploidy and genome evolution (Soltis P, Soltis DE, eds), pp 341–383. New York: Springer Heidelberg.

Prober DA, Rihel J, Onah AA, Sung RJ, Schier AF (2006) Hypocretin/orexin overexpression induces an insomnia-like phenotype in zebrafish. J Neurosci 26:13400–13410. CrossRef Medline

Rawashdeh O, de Borsetti NH, Roman G, Cahill GM (2007) Melatonin suppresses nighttime memory formation in zebrafish. Science 318:1144–1146. CrossRef Medline

Rihel J, Prober DA, Arvanites A, Lam K, Zimmerman S, Jang S, Haggarty SJ, Kokel D, Rubin LL, Peterson RT, Schier AF (2010) Zebrafish behavioral profiling links drugs to biological targets and rest/wake regulation. Science 327:348–351. CrossRef Medline

Rink E, Wullimann MF (2002) Development of the catecholaminergic system in the early zebrafish brain: an immunohistochemical study. Brain Res Dev Brain Res 137:89–100. CrossRef Medline

Rösler M, Retz W, Retz-Junginger P, Hengesch G, Schneider M, Supprian T, Schwitzgebel P, Pinhard K, Dovi-Akue N, Wender P, Thome J (2004) Prevalence of attention deficit-/hyperactivity disorder (ADHD) and comorbid disorders in young male prison inmates. Eur Arch Psychiatry Clin Neurosci 254:365–371. CrossRef Medline

Roybal K, Theobold D, Graham A, DiNieri JA, Russo SJ, Krishnan V, Chakravarty S, Peevey J, Oehrlein N, Birnbaum S, Vitaterna MH, Orsulak P, Takahashi JS, Nestler EJ, Carlezon WA Jr, McClung CA (2007) Mania-like behavior induced by disruption of CLOCK. Proc Natl Acad Sci U S A 104:6406–6411. CrossRef Medline

Ryu S, Mahler J, Acampora D, Holzschuh J, Erhardt S, Omodei D, Simeone A, Driever W (2007) Orthopedia homeodomain protein is essential for diencephalic dopaminergic neuron development. Curr Biol 17:873–880. CrossRef Medline

Tay TL, Ronneberger O, Ryu S, Nitschke R, Driever W (2011) Comprehensive catecholaminergic projectome analysis reveals single-neuron integration of zebrafish ascending and descending dopaminergic systems. Nat Commun 2:171. CrossRef Medline

Toh KL, Jones CR, He Y, Eide EJ, Hinz WA, Virshup DM, Ptácek LJ, Fu YH (2001) An hPer2 phosphorylation site mutation in familial advanced sleep phase syndrome. Science 291:1040–1043. CrossRef Medline

Tovin A, Alon S, Ben-Moshe Z, Mracek P, Vatine G, Foulkes NS, Jacob-Hirsch J, Rechavi G, Toyama R, Coon SL, Klein DC, Eisenberg E, Gothilf Y (2012) Systematic identification of rhythmic genes reveals camk1gb as a new element in the circadian clockwork. PLoS Genet 8:e1003116. CrossRef Medline

Vallone D, Gondi SB, Whitmore D, Foulkes NS (2004) E-box function in a period gene repressed by light. Proc Natl Acad Sci U S A 101:4106–4111. CrossRef Medline

VanGuilder HD, Vrana KE, Freeman WM (2008) Twenty-five years of quantitative PCR for gene expression analysis. Biotechniques 44:619–626. Medline

Wang H (2008) Comparative analysis of period genes in teleost fish genomes. J Mol Evol 67:29–40. CrossRef Medline

Wang H, Zhou Q, Kesinger JW, Norris C, Valdez C (2007) Heme regulates exocrine peptidase precursor genes in zebrafish. Exp Biol Med (Maywood) 232:1170–1180. CrossRef Medline

Wang L, Zhang P, Wei Y, Gao Y, Patient R, Liu F (2011) A blood flow-dependent klf2a-NO signaling cascade is required for stabilization of hematopoietic stem cell programming in zebrafish embryos. Blood 118: 4102–4110. CrossRef Medline

Westerfield M (1993) The zebrafish book: a guide for the laboratory use of zebrafish (Brachydanio rerio). Eugene, OR: University of Oregon.

Xu X, Breen G, Chen CK, Huang YS, Wu YY, Asherson P (2010) Association study between a polymorphism at the 3′-untranslated region of CLOCK gene and attention deficit hyperactivity disorder. Behav Brain Funct 6:48. CrossRef Medline

Yamada K (2011) Translational research in neurodevelopmental disorders: development of etiology-based animal models. Forward. Biol Pharm Bull 34:1357. CrossRef Medline

Zhu J, Lee KP, Spencer TJ, Biederman J, Bhide PG (2014) Transgenerational transmission of hyperactivity in a mouse model of ADHD. J Neurosci 34:2768–2773. CrossRef Medline